A Review on the Photovoltaic Panels: Applications, Modeling and Economic Evaluation with Focusing on the Phase Change Material Cooling Method

Seyyed Masoud Seyyedi[1,2*]

Abstract–A photovoltaic (PV) panel consists of several photovoltaic cells designed to convert solar radiation into electrical energy. Cooling of PV cells is an important task to increase PV panel efficiency, improve output power and optimize performance parameters. There are various methods for PV cooling. Phase change materials (PCMs) can be used to cool PV panels. The integrated system is called PV-PCM system. This paper provides an overview of the history, applications, mathematical modeling and economic evaluation for PV-PCM systems. The focus of this study is on the cooling of the PV cells using PCMs. Furthermore, the other types of PV systems (hybrid systems) are investigated. The effects of main parameters on the performance of PV or PV-PCM systems are investigated, too. Mathematical modeling including thermal and electrical models are presented. Finally, the advantages and disadvantages of PV-PCM system and its future overview are discussed. The results discover that the PV panel temperature up to 20 °C and electrical efficiency up to 5% can be reduced by PCM.

1. Introduction

Nowadays renewable energies (such as wind, solar, tidal, micro-hydro, geothermal and biomass) are more interested than fossil fuels (such as natural gas and coal) because the latter leads to pollution and greenhouse emissions. Specially, Solar energy is a reliable energy source. It is a free renewable energy source with no gas emissions [1].Solar energy can be applied to obtain electrical power directly using photovoltaic (PV) solar cells or indirectly using a solar thermal system. The PV systems can be divided into two categories, flat panel PV and concentrator PV, in terms of module geometry [2]. The solar towers, solar dishes and parabolic trough solar collectors (PTSC) are examples of solar thermal systems that can be applied to produce electrical power [3].Fig. 1 represents the main applications of solar energy.

1,2* Corresponding Author:
1Department of Mechanical Engineering, Aliabad Katoul Branch, Islamic Azad University, Aliabad Katoul, Iran.
 Email: s.masoud_seyedi@yahoo.com
2Energy Research Center, Aliabad Katoul Branch, Islamic Azad University, Aliabad Katoul, Iran

Solar PV electricity generation is practically preferable to solar thermal due to wider application scenarios [4]. PV systems are an excellent choice at a reasonable price for remote areas for low to medium power levels due to easy scaling of the input power source [5]. In fact, the main attraction of PV systems is that they generate electrical power by directly converting solar energy into electricity without harming the environment. Unfortunately, the price of a unit of energy produced from a PV system is higher than that of conventional energy supplied by the power grid to urban areas, because the technologies associated with PV power systems are not yet fully developed. However, the continuous reduction in the cost of PV arrays and increasing their efficiency have a promising role for PV generation systems in the near future.

1.1. Photovoltaic technology

The major contribution of solar radiation incident on the PV module cannot be converted into electricity. Only 5–20% of the incident solar energy is converted into electricity, depending on the PV cell technology and the remaining energy is converted into heat[6]. PV technology is based on the PV effect, which for the first time was discovered by Edmond Becquerel in 1839 [7]. It should be noted that PV effect occurs due to the absorption of photon energy over

the band gap. In 1883, Fritz developed the first PV cell and its efficiency was less than 1% where in 1954the first practical solar cell was constructed[8].Initially, the main goal of research on PV technology was to power space satellites. The energy crisis of the 1970s drew public attention to PVs and their potential to become an alternative municipal electricity source. PV cells (also called solar cells) made of semiconductor materials are the building block of a PV system. A number of solar cells connected electrically to each other to form a PV module. Multiple modules can be connected together to form an array. PV arrays can be connected in both parallel and series electrical arrangements to produce any required current and voltage combination. A PV system typically consists of the PV array and a number of supporting elements known as the balance of system (BOS). BOS refers to the components other than the module [2]. Fig. 2 represents the PV system and BOS. PV systems can be classified from different viewpoint that have been summarized in the Table 1. For more details, see Ref. [2].
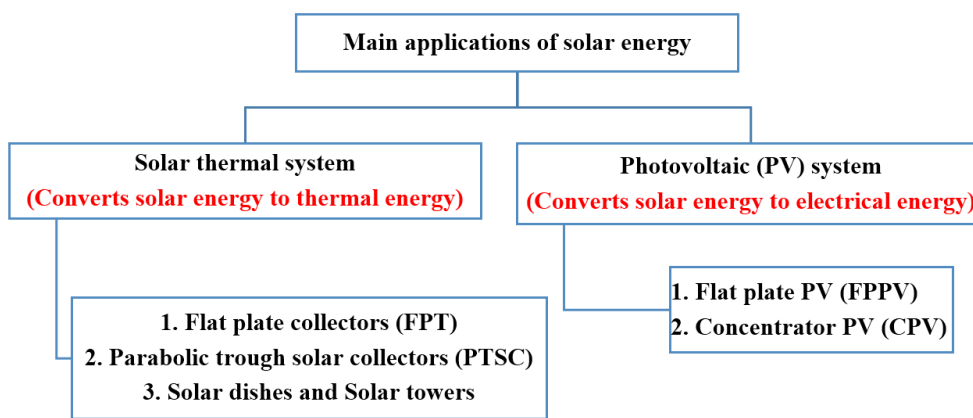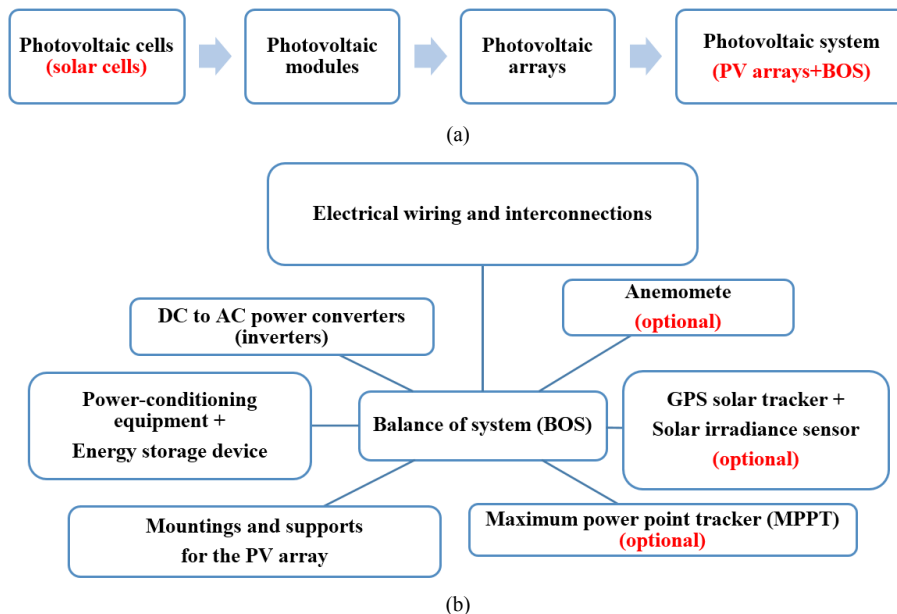
Fig. 1: The main applications of solar energy

Fig. 2:(a) Photovoltaic system and (b) BOS

Table 1:PV system taxonomy[2]

Basis of classification	PV denomination
PV cell materials	1. Silicon based PV
	I. Crystalline silicon PV
	a. Monosilicon (m-Si) PV
	b. Polysilicon (p-Si)
	II. Amorphous silicon (a-Si) PV
	a. Single junction
	b. Double junction
	c. Triple junction
	2. Group III-V material based PV
	3. Thin film solar cell (TFSC) based PV
	a. Si based PV
	b. CdS/CdTe based PV
	c. CIS/CIGS based PV
	4. Dye sensitized solar cell (DSSC) based PV
	5. Organic/Polymer based PV
Interfacing with load	1. Grid connected PV
	2. Off-grid or Standalone PV
Mode of installation	1. Building integrated PV (BIPV)
	2. Rack-mounted PV (RPV)
	3.Roof-top RPV
	4. Ground-mounted RPV
Tracking facility	1. Tracking system PV
	2. Fixed tilt PV
Module geometry	1. Flat plate PV (FPPV)
	2. Concentrator PV (CPV)
System complexity	1. Simple photovoltaic system (PV-only)
	2. Hybrid photovoltaic thermal system (PVT)

1.2. Photovoltaic performance

Solar PV panels are increasingly used worldwide due to their ability to operate under diffuse radiation. So, it is important to know how PV panels respond to changed climatic conditions. The PV efficiency is approximately 30% under laboratory conditions, but in real conditions, its value is only about 5–20%[9]. Different parameters can affect the efficiency, such as the dust accumulation on the PV surface and the solar radiation intensity. PV module efficiency decreases by approximately 0.40–0.65% when the module temperature increases by only 1 °C[10]. This fact has been reported extensively in previous works, for example [11, 12]. The PV temperature can reach to 80 °C and even higher than 100 °C in desert regions[6], that leads to a significant reduction in PV power generation. As we know, the amount of electricity produced from each unit of solar energy depends on the electrical and physical properties of PV cells and environmental conditions. While scientists are developing PV cells with higher conversion efficiency, the PV efficiency is constrained by its operating conditions [7].

Several PV cells make up a PV panel. Their task is to

convert solar radiation into electric energy. The performance of PV panels is determined as conversion efficiency or how much solar radiation [W/m^2] is transformed into electric power [W/m^2] in certain conditions. The electrical power conversion efficiency for commercial PV modules is conventionally between 13% and 20%[13]. Consequently, only a small part of the absorbed solar energy is converted to electricity whereas the remaining portion is converted into heat. This leads to increasing the temperature of PV panel. One of the most important factors that affect the efficiency of PV panels, is temperature. The PV module temperature is a function of its physical properties and environmental conditions. The temperature of a PV module has been modelled by various authors and a good literature review of these works is given in [14]. As we know, some of the sun's radiation is converted into electrical energy and most of it into thermal energy. This leads to PV cells heating up and reducing their electrical efficiency. There are different ways to reduce the temperature in PV panels. PV cooling techniques include passive techniques and active techniques, which are summarized in Fig. 3 [15]. These include air based, liquid-based and PCM based PV cooling systems. All these cooling techniques can be used actively and passively. The active system is more effective than passive system since it uses the water (or other coolants) as cooling fluid although it consumes more electricity and costs more. For more details, see Ref. [16]. Hasan et al. [17] have summarized the advantages and disadvantages of the PV thermal management technologies. Among the cooling techniques, the current paper focuses on the PCM-based PV cooling systems.
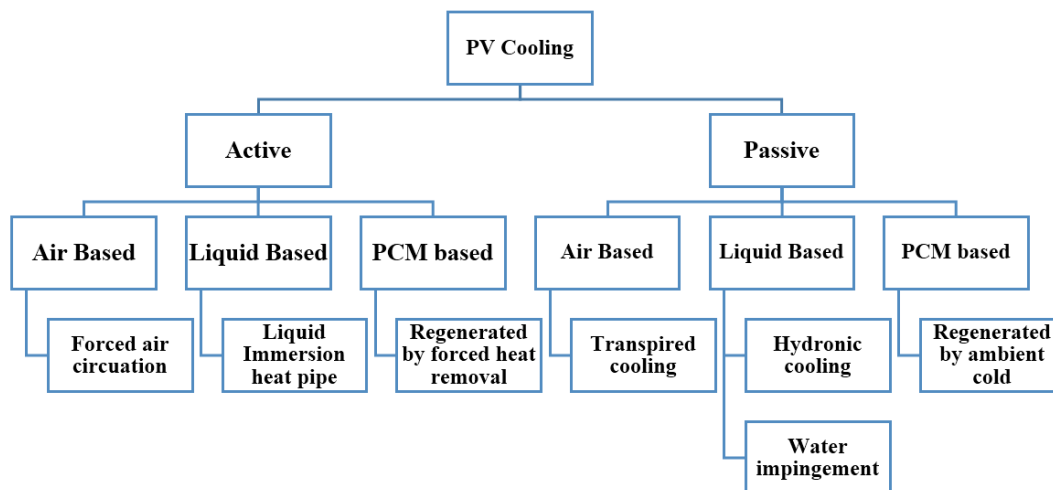

Fig. 3: Some PV cooling techniques [15]

1.3. PV cooling systems based on PCM

The main purpose of using thermal regulation techniques in PV panels is to reduce the temperature of the solar cells as low as possible and close to the standard test conditions (STC) in order to increase the efficiency [18]. STC will be introduced at section 3.One of the promising solar energy storage techniques is the use of phase change materials (PCM).A comprehensive review for solar energy storage using PCMs has been published by Kenisarin and Mahkamov[19].Thermal regulation of PV panel based on the PCM is classified as passive cooling technique [20]. This system is known as PV-PCM system. Research in PV-PCM systems are gaining interest. In these firstly, the solid PCM turns into liquid during sunny hours and then the reverse process occurs during non-sunny hours. on the other words, the absorbed heat is rejected to the ambient during non-sunshine hours[15].As we know, a lot of energy can be stored by a small amount of PCMs when they undergo a phase change. PCMs can be used in many industrial applications such as cooling electronic devices [21, 22], solar heating systems [23, 24],waste heat recovery [25, 26], and thermal energy storage systems [27, 28]. Unfortunately, they have low thermal conductivity and therefore, many researchers have tried to improve their thermal conductivity. Recently, the nano encapsulated phase change materials (NEPCMs) were proposed by scientists. NEPCMs are a new type of nanofluids that nanoparticle includes a shell

and a PCM core [29]. It should be mentioned that the conventional nanofluids are used to enhance heat transfer in many various industries such as solar collectors, radiators, air conditioning in buildings, cooling of electronic circuits and medical applications [30-32]. Nanofluids can be produced by adding the nano-sized particles (such as copper and silver) into the base fluids (such as oils, water, and so on) [33]. Simulation of their behavior in cavities is an interesting subject for researchers due to many industrial applications [34-41].Also, nanofluids can be applied as an effective coolant for PV modules. For example, Elmir et al. [42] and Yun and Qunzhi[43] used Al_2O_3-water and MgO-water, respectively, as a nanofluid for cooling the PV modules. Micro-Encapsulated PCM (MEPCM) was first time used for PV cooling by Ho et al. [44,45] and Tanuwijava et al. [46].On the other hand, NEPCMs simulation have been performed by some researchers [47-51]. Many experimental and theoretical studies have been published on PV-PCM cooling. In 1978, Stultz et al. [52] proposed to use PCM to cool the PV panel since PCM has the latent heat capacity which can absorb substantial amount of heat from PV. However, the first study on the PCM based cooling of PV panels was published in the year 2004 by Huang et al. [53]. They studied the thermal behavior of the PV-PCM system using a 2-D numerical model. They studied three different systems experimentally and numerically. In order to simulate a PV cell, they applied an aluminum plate. An aluminum plate attached to a chamber filled with PCM was used to simulate a PV-PCM system. The third system was a PV-PCM system including internal fins. They discovered that the temperature of PV cell can reduce more than 30 °C when the internal metal fins are attached to the PCM chamber [54]. Literature shows that PCM can effectively reduce the temperature of the PV panel by 20°C and also improve the electrical conversion efficiency by 5% [15, 55-57]. A PV-PCM system with aluminum fins studied theoretically and experimentally by Huang et al. [58- 60]. Hasan et al. [17]studied experimentally, the effect of PCM thermal properties such as thermal conductivity and melting point on PV surface temperature under different solar radiation. They concluded that PCMs with higher conductivity and higher melting point are better for the PV operating at high temperature. With the PCM application, a performance increase between 2.5% and 10.7% have been achieved in the PV panel power output [61,62]. In a study PCMs to

reduce the operating temperature of the PV panel, higher performance was obtained compared to a conventional PV module, especially during the hottest months. They showed that 3.5–10% more electrical energy could be obtained from a PV panel using PCM all year long [63].In 2014, a techno-economic study on the PV-PCM system for two locations with different climates was conducted by Hasan et al. [64].In 2014, Park et al. [65] studied a PV-PCM in South Korea and concluded that electricity production can be improved by 1–1.5% annually using PCM. In 2017, a year-round numerical study conducted in United Arab Emirates suggests that in extremely hot climate, the PV-PCM system can raise the annual electricity yield by 5.9% [66].In 2009, an enhanced thermal conduction model for the prediction of convection dominated solid–liquid phase change was proposed by Vidalain et al. [67]. In 2013, annual performance enhancement of building integrated PV modules by applying PCM was investigated by Hendricks and Sark[68].In 2013, the thermal energy storage technologies and concentrating solar power (CSP) systems including PCMs were analyzed by Kuravi et al. [69]. In 2013, Du et al. [70] made a critical review on the thermal management systems for crystalline silicon based PV panels in which PV-PCM systems are highlighted as a prospective method. In 2012 and 2014, the finite difference thermal model was applied for a PV-PCM system by Ciulla et al. [71] and Brano et al. [72], respectively. In 2014, the thermal regulation systems including PCMs (PV-PCM) for electronic components and Li-ion batteries were extensively studied by Ling et al. [21]. In 2015, Atkin and Farid [20] studied improving the efficiency of PV cells using PCM. They used aluminum fins. In 2015, Browne et al. [15]performed a review on the application of PCM in PV systems and analyzed the economic viability of PV-PCM systems. Also in 2015, Zhou et al. [73] reviewed on the use of PCMs for solar thermal energy storage in residential buildings in cold climate. In 2015, a good review paper on the use of PCMs in PV systems for thermal regulation has been published by Ma et al. [74]. In 2016, Kant et al. [75] studied the heat transfer of PV panel coupled with PCM. In 2016, Stropnik and Stritih [55] used TRNSYS software for modeling the PV-PCM system. They verified modeling results with the outdoor experimental results. In 2016, Bahaidarah et al.[76]studied the various uniform cooling techniques for PV panels including PCM systems. In 2016, another good review paper has been

published by Islam et al. [2]. They reviewed recent advances and achievements in PV-PCM technology. In 2017, a parametric study about the potential to integrate PCM into PV panel was performed by Ma et al. [77]. In 2018, the mathematical model of the PV-PCM system was developed by Ma et al. [78]. They compared the1-D thermal resistance model and the CFD model to each other. In 2018, a review paper on the thermal and electrical management of PV panels using PCMs was published by Waqas et al. [16]. They mentioned the names of PCMs used for cooling of PV [see Table 3 from Ref.16].Also, they reported that approximately 2.6 kg of PCM per 1 m² of PV panel area is required to reduce the PV panel temperature by 1℃ during peak hours.In 2019, the year-round performance analysis of a PV panel coupled with PCM was performed by Zhao [79]. In 2019, Ma et al. [80] performed a research review on the application of PCMs in PV system. In 2020, Savvakis et al. [81]studied the operational performance of an alternative PV-PCM concept. In 2021, Sharma and Gaur [82]published a good review paper on the application of PCMs for cooling of solar PV panels. The rest of paper are organized as follows:

Section 2 provides the configuration of system. The mathematical modeling including electrical model, solar radiation model and electricity generation model will be presented in section 3. The effectiveness of PCM for thermal and electrical regulation of PV panel will be discussed in section 4. Section 5 presents the hybrid PV systems. Economic feasibility of PV-PCM systems are shown in section 6. The effects of main parameters on the performance of PV or PV-PCM systems will be investigated in section 7. Finally, future developments and a short summary are presented in sections 8 and 9,

respectively. More than one hundred forty publications are reviewed in this study.

2. System configuration

As mentioned earlier, it has been reported that when the PV temperature increases by only 1°C, the output power can be decrease by 0.4-0.65%. PCM can be employed to control PV module temperature and increase power generation since it can absorb great amount of heat without raising the temperature of itself. This kind of integrated system is the so-called PV-PCM system[78].Basically, PV-PCM system has two significant parts, i.e. PV panel and PCM container (or called PCM chamber). Usually, crystalline silicon PV is used in the system because it has a high temperature coefficient and wide applications[74]. There are several geometrical configurations of PCM chamber such as rectangle chamber, semi-circle chamber, triangle chamber, finned chamber and so on [70, 83]. But, generally rectangle chamber is selected [78]. Conventional PV panels have different layers depending on the type of design and manufacturing technology[84]. Conventionally, the main layers are: exterior glass, ARC (anti reflexive coating), PV cells (silicon cells), EVA (ethylene-vinyl acetate), metal rear contact and tedlar [13].Fig. 4 represents an example of the PV-PCM system that is assembled by a PV module and an aluminum chamber filled with PCM. Fins in the aluminum chamber is optional. RT35 has been considered as the PCM since it is commercially available, non-combustible and non-corrosive [17, 85]. Table 2summarizes the basic properties of PV-PCM system [78].
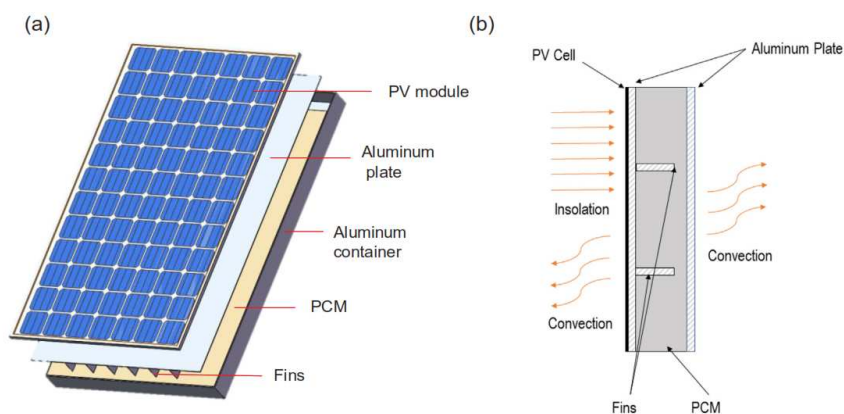

Fig. 4:(a) 3-D view of PV-PCM system; (b) schematic of the system configuration. [78]

Table 2: The properties of PV module and PCM chamber[78]

Property	Glass	EVA	Silicon cells	Tedlar	Polyester	RT35 (PCM)	Aluminum
Density (kg/m^3)	2500	935	2330	1500	1390	800	2791
Specific heat(J/(kg K))	750	2500	700	1090	1172	2000	871
Thickness(mm)	3.2	0.5	0.2	0.0375	0.25	20-50	5
Thermal conductivity(W/(m K))	1.04	0.29	150	0.35	0.155	0.2	202.4
Emissivity	0.95	-	-	-	-	-	0.095
Solidus temperature(℃)	-	-	-	-	-	29	-
Liquids temperature (℃)	-	-	-	-	-	36	-
Latent heat capacity (kJ/kg)	-	-	-	-	-	130	-

3. Mathematical model

A multi-physics model must be performed to investigate the thermal behavior of a PV panel when it works under variable environmental conditions.

3.1.Electricalmodel

In a PV panel, the PV cells are mounted in arrays connected in series and/or parallel to produce the desired output voltage, current or power. The one-diode model, can be used to describe the electrical behavior of a PV panel [86]. Fig. 5 represents a typical electrical circuit of the solar PV cell[87]. Based on this model, the voltage and current relationship can be given as follows (Kirchhoff's law of current) [88]:
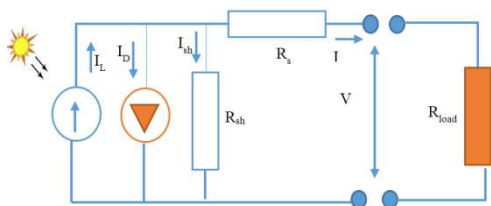

Fig. 5: Equivalent electrical circuit in the five-parameter photovoltaic model (reproduced from Ref. [87])

$$I = I_L - I_D - I_{sh} = I_L - I_0\left(\exp\left(\frac{V + IR_s}{a}\right) - 1\right) \\ - \frac{V + IR_s}{R_{sh}} \tag{1}$$

where$V$ is the voltage/potential at the terminals of the circuit,I is the current and I_L is the current source,I_0 is the diode reverse saturation current, R_{sh} is the shunt

resistance,R_s is the series resistance and$a$ a modified diode ideality factor given by the following relation:

$$a = \frac{N_s k_B \alpha_n T_c}{q_e} \tag{2}$$

where N_s is the number of PV cells connected in series, k_B is the Boltzmann constant($k_B = 1.38 \times 10^{-23}$J/K), α_n is the diode ideality factor (for an ideal diode, it is equal to 1 and for an non-ideal diode is between 1 and 2 [87]), T_c is the operating temperature of the PV cells and the constant q_e is the electron charge($q_e = 1.602 \times 10^{-19}$C).

It should be mentioned that Eq. (1) can be expanded for PV panels with strings of cells connected in parallel. In 2013, Tsai [89] proposed the following expression for electrical model:

$$I = N_p I_L - N_p I_0\left(\exp\left(\frac{q_e}{k_B \alpha_n T_c}\left(\frac{V}{N_s} + \frac{IR_s}{N_p}\right)\right) - 1\right) \\ - \frac{(N_p/N_s)V + IR_s}{R_{sh}} \tag{3}$$

whereN_s and N_p are the number of cells connected in series and parallel inside the PV panel, respectively.

A PV array is nonlinear component and can be interpreted by its current-voltage $(I - V)$ characteristic curve. Also, it is worth noting that there are different mathematical models, which can describe I-V characteristic curve. Eq. (1), represents the five-parameter photovoltaic model(a, I_L, I_0, R_s andR_{sh}) for I-V characteristic curve [90]. The current-voltage $(I - V)$ curve of a solar cell is a nonlinear inclination that gives three important parameters: the short-circuit current I_{sc}, the open-circuit, voltage V_{oc},,

and the maximum power point P_{max}. Fig. 6 shows an example of current-voltage curve for a solar cell. To determine these parameters (I_{sc}, V_{oc} and P_{max}) some reference conditions are needed [90]:
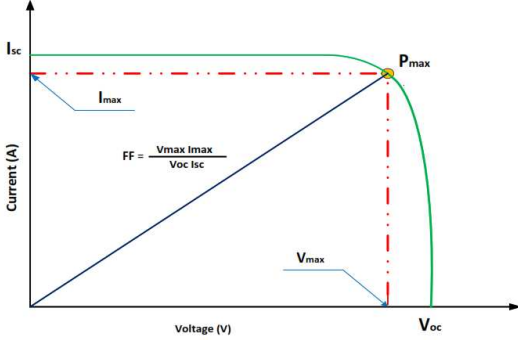

Fig. 6: Representation of current-voltage curve of solar cell.

At short circuit current:

$$I = I_{sc,ref} \text{ and } V = 0 \tag{4}$$

At open circuit voltage:

$$I = 0 \text{ and } V = V_{oc,ref} \tag{5}$$

At the maximum power point:

$$I = I_{mp,ref} \text{ and } V = V_{mp,ref} \tag{6}$$

At the maximum power point:

$$\left[\frac{d(IV)}{dV}\right]_{mp} = 0 \tag{7}$$

At short circuit:

$$\left[\frac{dI}{dV}\right]_{sc} = -\frac{1}{R_{sh}} \tag{8}$$

Substituting the Eqs. (4-8) into Eq. (1) generate five nonlinear equations that must be solved with numerical methods. Solving of them gives the value of five parameters (a_{ref}, $I_{L,ref}$, $I_{0,ref}$, $R_{s,ref}$ and $R_{sh,ref}$) at the reference conditions. For calculation the model parameters at new climatic and operating conditions (G_{new}, $T_{cell,new}$) a set of auxiliary equations is used [91,92]. For more details, see Ref. [90].

According to Fig. 6, the maximum output power of a

solar cell can be described graphically as the largest rectangular area that can be fitted under the $(I-V)$ curve:

$$P_{mp} = V_{mp} I_{mp} \tag{9}$$

Where V_{mp} and I_{mp} define the maximum voltage and current, respectively.

➤ *Reference conditions*

Because the power of a PV cell is dependent on solar irradiation level and temperature changes, the standard parameters are defined that can generate the Watt-peak (W_p). Therefore, the electrical power generated by a PV panel (measured in W_p) is evaluated at reference conditions or standard test conditions (STCs). The average temperature of solar cell $(T_{cell,ref})$, the solar radiation intensity (G_{ref}) and wind speed $(u_{wind,ref})$ at STCs are 25°C, 1000 W/m² and 1 m/s, respectively [84].

➤ Fill factor (FF)

The fill factor (FF) is the ratio of the maximum power produced by a solar cell to the product of I_{sc} and V_{oc} [93]:

$$FF = \frac{V_{mp} I_{mp}}{V_{oc} I_{sc}} \tag{10}$$

➤ Energy efficiency

The energy efficiency (or actual electrical efficiency) of a PV system at maximum power is defined as the ratio of actual electrical output to input solar energy incident on PV surface area and it is given by [93, 94]

$$\eta_{el} = \frac{V_{mp} I_{mp}}{S} = \frac{FF \, V_{oc} I_{sc}}{S} \tag{11}$$

It should be mentioned that the maximum energy efficiency of a PV system is given by [94]:

$$\eta_{el,max} = \frac{V_{oc} I_{sc}}{S} \tag{12}$$

Therefore, we have:

$$\eta_{el} = FF \, \eta_{el,max} \tag{13}$$

In Eq. (11), S is solar absorbed flux (W) and it is given by [90, 93]

$$S = G \, A_{arr} = G(N_s N_m A_{mod}) \tag{14}$$

where G, A_{arr}, N_m and N_s are solar radiation

intensity (W/m^2), PV array area, number of modules in series per string, and number of strings, respectively. PV module area (A_{mod}) can be calculated by:

$$A_{mod} = L \times W \tag{15}$$

where L and W are the length and width of solar module, respectively.

3.2. Exergy Analysis

Exergy is one of the important concepts of the second

lawof thermodynamics, which is the maximum useful work that wecan obtain from a flow of matter or energy [95]. Exergy efficiency is defined as the ratio of total output exergy to total input exergy [96]:

$$\eta_{ex} = \frac{Ex_{out}}{Ex_{in}} = 1 - \frac{I_{c.v}}{Ex_{in}} \tag{16}$$

The main equations for exergy analysis are summarized in Table 3.

Table 3: The main equations for exergy analysis

Descriptions	Equations	No.
The inlet exergy is exergy of solar radiation intensity. According to the Petela theorem, it can be calculated by Eq. (17), [97, 98]. T_{sun} stands for the effective temperature of the sun, which Holmberg et al. [99] estimated to be 5777.	$Ex_{in} = S\left[1 - \frac{4}{3}\frac{T_{amb}}{T_{sun}} + \frac{1}{3}\left(\frac{T_{amb}}{T_{sun}}\right)^4\right]$	(17)
The irreversibility of control volume is sum of the external exergylosses and internal exergy losses (exergy destructions). [90]:	$I_{c.v} = \sum(Ex_{loss} + Ex_{dest})$	(18)
The external exergy loss due to heat leakage is obtained by Eq. (20) [100]:	$Ex_{loss} = U_L A_{arr}(T_{cell} - T_{amb})\left(1 - \frac{T_{amb}}{T_{cell}}\right)$	(19)
The exergy destruction includes four terms; the first term is due to optical losses in PV array surface [90]:	$Ex_{dest,opt} = S\left(1 - \frac{T_{amb}}{T_{sun}}\right)(1 - (\tau\alpha))$	(20)
The second term is caused by the temperature difference between PV array surface and the sun temperature [101]:	$Ex_{dest,\Delta T_{sun}} = (\tau\alpha)ST_{amb}\left(\frac{1}{T_{cell}} - \frac{1}{T_{sun}}\right)$	(21)
The third term is due to the temperature variation of PV panel with respect to the ambient temperature [100,101]:	$Ex_{dest,\Delta T_{arr}} = \frac{m_{cell}C_p T_{amb}}{\Delta t}\left(\ln\left(\frac{T_{cell}}{T_{amb}}\right) - \frac{(T_{cell} - T_{amb})}{T_{cell}}\right)$	(22)
The specific heat capacity of silicon solar cell (C_p) can be obtained using Eq. (23)[90]:	$C_p = 0.844 + 1.18 \times 10^{-4}T_{cell} - 1.55 \times 10^4 T_{cell}^{-2}$	(23)
The fourth term is electrical exergy destruction [94]:	$Ex_{dest,el} = I_{sc}V_{oc} - I_{mp}V_{mp}$	(24)

3.3. Solar radiation model

The solar radiation model is used to calculate the amount of absorbed solar radiation(G in Wm^{-2}) by PV cells which can be estimated by the following equation [102]:

$$G = (\tau_{fg}\alpha_{PV})_n G_T \tag{25}$$

where $(\tau_{fg}\alpha_{PV})_n$ is the normal transmitivity-absorptivity product [86].G_T(W/m^2) is solar radiation of the surface of the PV panel and can be obtained by:

$$G_T = R_b G_b K_b + G_d K_d\left(\frac{1 + \cos\beta}{2}\right) + (G_b + G_d)\rho_{ground}K_{ground}\left(\frac{1 - \cos\beta}{2}\right) \tag{26}$$

Other necessary equations for solar radiation modeling

are summarized in Table 3 based on different angles of a PV panel shown in Fig. 7.In Eq. (26), G_b(W/m^2) and G_d(W/m^2) are direct (beam) and diffuse solar radiations on horizontal plane, respectively. Also, the other parameters of Eq. (26), are given in Table 4.
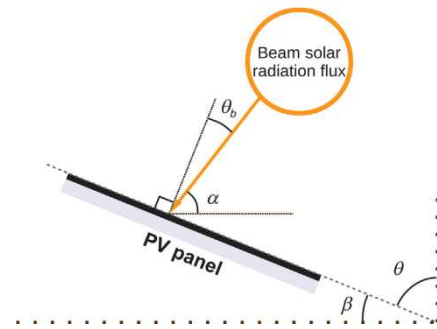

Fig. 7: Angles in a PV panel[86]

Table 4: Solar radiation modeling[86]

Definition of parameter	Equation	No.
The tilt angle of the PV panel (β)	Shown in Fig. 7	-
The ratio of beam radiation on the tilted plane to that on the horizontal plane (R_b)	$R_b = \dfrac{\sin(\alpha + \beta)}{\sin(\alpha)}$	(27)
The elevation angle (α) where φ is the latitude of the location	$\alpha = 90 - \varphi + \delta$	(28)
The declination angle (δ) where d is day of year	$\delta = 23.45 \sin\left[\dfrac{360}{365}(284 + d)\right]$	(29)
The incidence angle modifier for the beam radiation (K_b) where $b_o = -1$	$K_b = 1 + b_o\left(\dfrac{1}{\cos(\theta_b)} - 1\right)$	(30)
The incidence angle of the beam solar radiation on the surface of the PV panel (θ_b)	$\theta_b = 90 - (\alpha + \beta)$	(31)
The incidence angle modifier for the diffuse radiation (K_d)	$K_d = 1 + b_o\left(\dfrac{1}{\cos(\theta_d)} - 1\right)$	(32)
The incidence angle modifier for the ground-reflected radiation (K_{ground})	$K_{ground} = 1 + b_o\left(\dfrac{1}{\cos(\theta_{ground})} - 1\right)$	(33)
The incidence angle for the diffuse radiation (θ_d)	$\theta_d = 59.68 - 0.1388\beta + 0.001497\beta^2$	(34)
The incidence angle for the ground-reflected radiation (θ_{ground})	$\theta_{ground} = 90 - 0.5788\beta + 0.002693\beta^2$	(35)
Reflectivity of the ground, also called albedo (ρ_{ground})	$\rho_{ground} = 0.2$	(36)

As mentioned above, the PV temperature (T_{PV}) depends on the solar radiation intensity on the module (G_T in Wm^{-2}), the wind velocity (u_{wind}), the ambient temperature (T_{amb}), the PV inclination, the PV module technology and structure, and the geometry of the PV modules with respect to wind direction.

3.4. Power generation model

The effect of PV temperature on its efficiency and power can be calculated by Eqs. (37) and (38), respectively [103, 104]:

$$P_m = \eta_{ref} G_T \left[1 - \beta_{cell}\left(T_{cell} - T_{ref}\right) + Y_{cell} ln\left(\frac{G_T}{G_{ref}}\right)\right] \tag{37}$$

$$\eta_{PV} = \eta_{ref}\left[1 - \beta_{cell}\left(T_{cell} - T_{ref}\right) + Y_{cell} ln\left(\frac{G_T}{G_{ref}}\right)\right] \tag{38}$$

P_m is Power generation (W/m^2), η_{ref} is conversion efficiency at standard conditions (conventionally, it takes values between 0.13 and 0.20 and is given by the PV panel manufacturer), G_T is total solar radiation on the tilted surface of the PV panel (W/m^2), T_{cell} is average temperature of the PV cell layer in °C, β_{cell} is temperature coefficient of the PV cell (it takes values between 0.4 %/K and 0.5 %/K and is usually provided by the PV panel manufacturer), Y_{cell} is solar radiation coefficient of the PV cell. $Y_{cell} = 0.085$ for single crystalline silicon cells, and $Y_{cell} = 0.11$ for poly-crystalline silicon cells [103]. Here, $T_{ref} = 25\,°C$ and $G_{ref} = 1000\ \text{W/m}^2$.

➤ *Necessary information*

It should be mentioned that hourly meteorological data over a complete year will be supplied by ENSERV for different locations. It is assumed that the following information will be provided:

- Latitude of the location (φ)
- Hourly data of direct solar radiation on horizontal plane (G_b)
- Hourly data of diffuse solar radiation on horizontal plane (G_d)
- Hourly data of air temperature (T_{air})
- Hourly data of wind velocity (u_{wind})

To calculate the total solar radiation on the surface of the PV panel, the solar radiation model must be used (See Table 4) assuming best orientation of the PV panel (south-oriented in North latitudes; north-oriented in South latitudes).

3.5. Mathematical modeling of PV-PCM system

For PV-PCM systems, different modelling methods can

be found in literature, including CFD model [105], thermal resistance model [106] and finite element model [107]. Also, an improved thermal resistance model by using enhanced conductivity method was developed for incorporation of PCM convective effect in 1-D model by Ma et al [78]. This innovative model offers a good compromise between simplicity and accuracy(The model will be discussed at subsection 3.5.5). For a typical PV-PCM system, the mathematical model can be generally divided into four main sections, i.e. heat transfer model, fluid model, phase change model and power generation model. Heat transfer model, fluid model and phase change model are commonly called thermal model. The aim of this subsection is to present a numerical model to simulate the thermal behavior and electricity production of a PV-PCM system on an annual basis. The model will be able to solve one dimensional (1D) heat transfer equations coupled with power generation equations from the following inputs:

- PV panel characteristics (geometry, layers properties, power generation efficiency).
- PCM layer properties and thickness.
- Hourly weather data, including at least direct solar radiation, global or diffuse solar radiation, air temperature, and wind velocity.
- Latitude of the location.

The outputs (hourly data) of the model will be:
- Time evolution of the temperature within the PV panel layers and PCM layer.
- Power generation.

The schematic view of a PV-PCM system is shown in Fig. 8. The properties of PV module and PCM chamber for Fig. 8 can be found in Table 1 from Ref. [79]. They are similar to the data presented in Table 2.
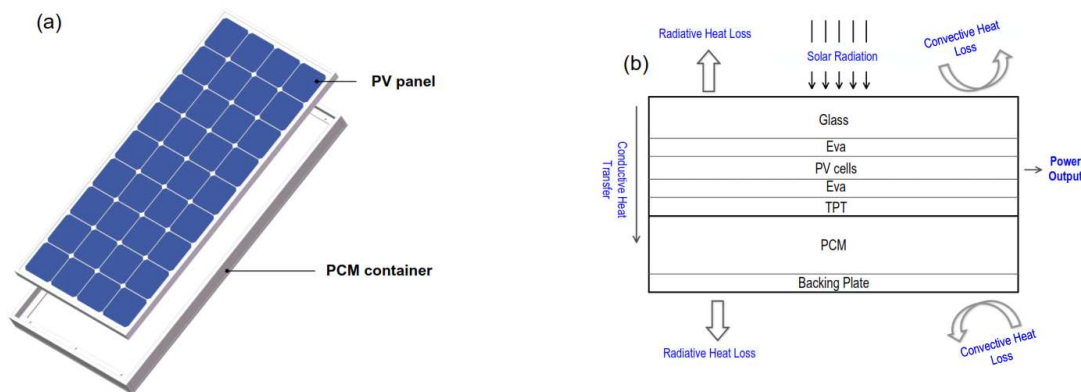

Fig. 8:(a) System configuration; (b) heat transfer pathway[79]

3.5.1. *Assumptions*

In the thermal model the following assumptions are made:

- Considering that the thickness of the PV panel is low comparatively to the surface of the panel, 1D heat transfer can be assumed.
- Assuming that a solid-solid PCM or a shape-stabilized PCM is used, the only heat transfer mechanism within the PCM layer is heat conduction.

- Phase transition of PCM occurs in a narrow range of temperatures and can be describe through currently used simplified enthalpy-temperature models.
- The thermal contact between any two layers of the PV-PCM system is assumed to be perfect. Therefore, equality of temperature and continuity of heat flux conditions apply at the interfaces between any two layers.

3.5.2. *Heat transfer equation*

The heat transfer equation within any layer of the PV-

PCM panel can be written as follows:

$$\rho c_p \frac{\partial T(x,t)}{\partial t} = k \frac{\partial^2 T(x,z)}{\partial x^2} + q \tag{39}$$

where ρ is the density of the material of the layer, c_p is the specific heat and k the thermal conductivity. All these parameters are assumed to be constant except the c_p value of the PCM layer, which is given by the temperature derivative of the PCM enthalpy function ($c_p = dH/dT$). The source term q is zero in all the layers expect in the glass cover and in the PV cell layers.

3.5.3.   *The boundary conditions*

1. The boundary condition on the top of the PV-PCM system (top of the glass layer) isas follows:

$$k_g \frac{\partial T_g}{\partial x}\bigg|_{front} = h_{front}\left(T_{g,front} - T_{air}\right) \tag{40}$$
$$+ F_{g-sky}\sigma\varepsilon_g\left(T_{g,front}^4 - T_{sky}^4\right)$$
$$+ F_{g-ground}\sigma\varepsilon_g\left(T_{g,front}^4 - T_{ground}^4\right)$$

where k_g and ε_g are, respectively, the thermal conductivity of the glass and its infrared emissivity. $T_{g,front}$, T_{air} and T_{ground} are the temperatures at the top surface of the glass layer, the air temperature and the ground temperature. σ is the Stefan–Boltzmann constant($\sigma = 5.67 \times 10^{-8}\text{W m}^{-2}\text{K}^{-4}$).

2. The boundary condition on the bottom of the PV-PCM system (bottom of the backing plate) is as follows:

$$k_b \frac{\partial T_b}{\partial x}\bigg|_{rear} = h_{rear}\left(T_{b,rear} - T_{air}\right) \tag{41}$$
$$+ F_{b-sky}\sigma\varepsilon_g\left(T_{b,rear}^4 - T_{sky}^4\right)$$
$$+ F_{b-ground}\sigma\varepsilon_b\left(T_{b,rear}^4 - T_{ground}^4\right)$$

where k_b and ε_b are, respectively, the thermal conductivity of the bottom layer of the system and its infrared emissivity. $T_{b,rear}$, T_{air} and T_{ground} are the temperatures at the rear face of the PV-PCM system, the air temperature, and the ground temperature.

To estimate the sky temperature, the following equations have been used in previous studies [86, 108]:

$$T_{sky} = 0.0552\, T_{air}^{1.5} \quad\text{or}\quad T_{sky} = 0.0375\, T_{air}^{1.5} + \tag{42}$$
$$0.32\, T_{air}$$

The ground temperature, can be assumed to be equal to the air temperature [86]:

$$T_{ground} = T_{air} \tag{43}$$

For the estimation of the convective heat transfer coefficient h_{front}, and h_{rear} there are different methods that have been proposed. According to SanchezBarroso et al. [86], it seems that the method proposed by Amstrong and Hurlay [13] provides the best agreement with experiments. (see, Table 5). Other necessary equations for thermal modeling are summarized in Table 5.

3. At the initial time ($t = 0$), the PV-PCM system is assumed to be in thermal equilibrium with the environment. That is, $\forall x, T(x, 0) = T_{air}$.

Table 5: Thermal modeling

Definition of parameter	Equation	No.
For glass cover layer: where e is the thickness of the glass cover and α_{glass} represents its solar absorptivity.	$q = \dfrac{\alpha_{glass} G_T}{e}$	(44)
For PV cell layer: WithP_m and G_T given by Eqs.(37) and (38) respectively. e is the thickness of the PV cell and $(\tau\alpha)_{eff}$ represents the effective product of transmissivity of glass cover and absorptivity of solar cell.	$q = \dfrac{(\tau\alpha)_{eff} G_T - P_m}{e}$	(45)

The view factor coefficients for glass to sky [86]

$$F_{g-sky} = \frac{1 + \cos \beta}{2} \tag{46}$$

The view factor coefficients for glass to ground[86]

$$F_{g-ground} = \frac{1 - \cos \beta}{2} \tag{47}$$

The view factor coefficients for rear to sky [13]

$$F_{b-sky} = \frac{1 + \cos (\pi - \beta)}{2} \tag{48}$$

The view factor coefficients for rear to ground[13]

$$F_{b-ground} = \frac{1 - \cos (\pi - \beta)}{2} \tag{49}$$

The forced convection coefficient $(Wm^{-2}K^{-1})$[109]

$$h_{conve-forced} = 11.4 + 5{,}7u_{wind} \tag{50}$$

The forced convection coefficient $(Wm^{-2}K^{-1})$ [Test et al. [110]

$$h_{conve-forced} = 8.55 + 2.56u_{wind} \tag{51}$$

Note: Any of the Eqs. (50) or (51) can be used.
The free convection coefficient $(Wm^{-2}K^{-1})$

$$h_{conve-free} = \frac{Nu \times k_{air}}{L_{PV,panel}} \tag{52}$$

where k_{air} is the air thermal conductivity ,Nu is the Nusselt number, and $L_{PV,panel}$ is the longest dimension of the PV panel.

The free (natural) convection from the top of the PV panel is obtained by Eq. (53)[111]:

$$\overline{Nu} = 0.14[(Gr \times Pr)^{1/3} - (Gr_{cr} \times Pr)^{1/3}] + 0.56(Gr_{cr} \times Pr \times \cos \theta)^{1/4} \tag{53}$$

where Pr is the Prandtl number,Gr and Gr_{cr} are the Grashof number and the critical Grashof number, respectively, and θ is the angle of inclination of the PV panel with the vertical (see Fig. 7).

For the critical Grashof number, see Refs. [13] and [111].

Natural convection from the bottom of a heated inclined plate is given as a function of the Nusselt number[112]:

$$\overline{Nu} = \left[0.825 + \frac{0.387 \times Ra^{1/6}}{[1 + (0.492/Pr)^{9/16}]^{8/27}}\right]^2 \tag{54}$$

Rayleigh number (Ra) is defined as [112]:

$$Ra = Gr\,Pr \tag{55}$$

Grashof number (Gr) is defined as [112]:

$$Gr = \frac{g\beta_t(T_{cell} - T_a)L^3}{\nu^2} \tag{56}$$

The effective convection heat transfer coefficient from the front surface of the PV panel (h_{front})

$$h_{front} = h_{conv} = \sqrt[3]{h_{conve-forced}^3 + h_{conve-free}^3} \tag{57}$$

The convection heat transfer coefficient from the rear surface of the PV panel (h_{rear})

$$h_{rear} = h_{conve-free} \tag{58}$$

3.5.4. *Simulation results*

Solving Eqs. (39)-(41) with hourly meteorological data and using Eq.(37) for power generation calculations, the following hourly data are produced:

- Temperature at any point within the PV-PCM system
- Power generated by the PV-PCM system.

However, for analysis purposes and comparisons, it is convenient to reduce them to some significant performance indicators:

- Total power produced by month.
- Total power produced by year.
- Maximum daily temperature

3.5.5 *Improved thermal resistance model*

An improved 1-D thermal resistant model was developed by Ma et al. [78]. The schematic view of 1-D thermal resistance model is shown in Fig. 9. The model consumes less computation time than CFD method. It can consider the effect of convective heat transfer within melted PCM using applying the enhanced conductivity method. Therefore, the enhanced conductivity model of PCM was proposed by Ma et al.[78]. The heat transfer rate k_{PCM} inside the PCM can be obtained by:

$$k_{PCM} = \begin{cases} k_{solidus} & if \ T < T_s \\ k_{solidus} + \dfrac{k_{liquidus}}{1 + \exp\left[-\dfrac{\xi\left(T - \frac{T_l + T_s}{2}\right)}{(T_l - T_s)}\right]} & if \ T_s < T < T_l \\ (k_{solidus} + k_{liquidus})(T_n - T_{n+1})^\omega & if \ T \geq T_l \end{cases} \tag{59}$$

where $k_{solidus}$ and $k_{liquidus}$ are the heat conductivity of solid and liquid PCM in $(W\,m^{-1}K^{-1})$; respectively. ξ and ω are constants that dependent on the property of PCM.T_n and T_{n+1} is the temperature of two adjacent PCM layers in°C. Fig. 10 represents the thermal conductivity of RT35(k_{PCM}) based on Eq. (59). For PCM of RT35, the

values of ξ and ω are 10 and 2, respectively [78]. Fig. 10 is corresponding to PV-PCM system that earlier was shown in Fig. 4 and Table 2.
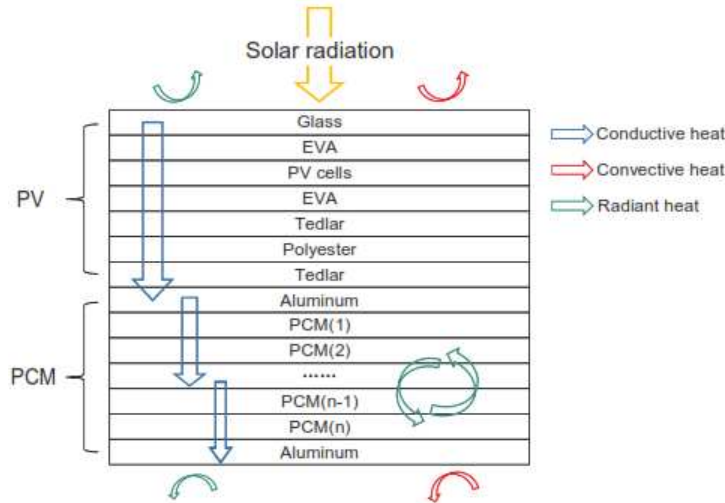

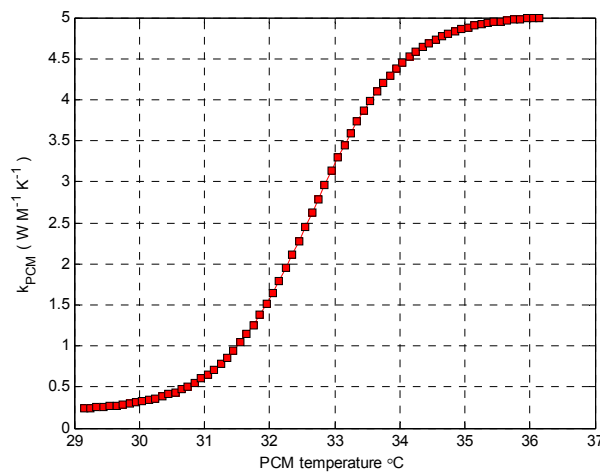**Fig. 9:** Schematic diagram of improved 1-D thermal resistance model [78]

Fig. 10: The variation of k_{PCM} versus temperature (recalculated from Ref. [78])

3.6. Experimental system design

Fig. 11shows a set of an experimental design for the PV-PCM system. The system consists of a PV panel, a battery, a dump load, a maximum-power-point tracker (MPPT) controller, the PT-100 temperature sensors and an analog data collector. More details about this structure can be found in the work of Zhao et a.[79, 113].

The aim of using PCM with PV panel is to reduce operating temperature of the PV panel and increase the electrical efficiency. Table 6 represents the main terms that must be used to evaluate the effectiveness of PCMs. Also, Waqas et al. [16] have summarized the findings of various studies related to PCMs in PV systems.

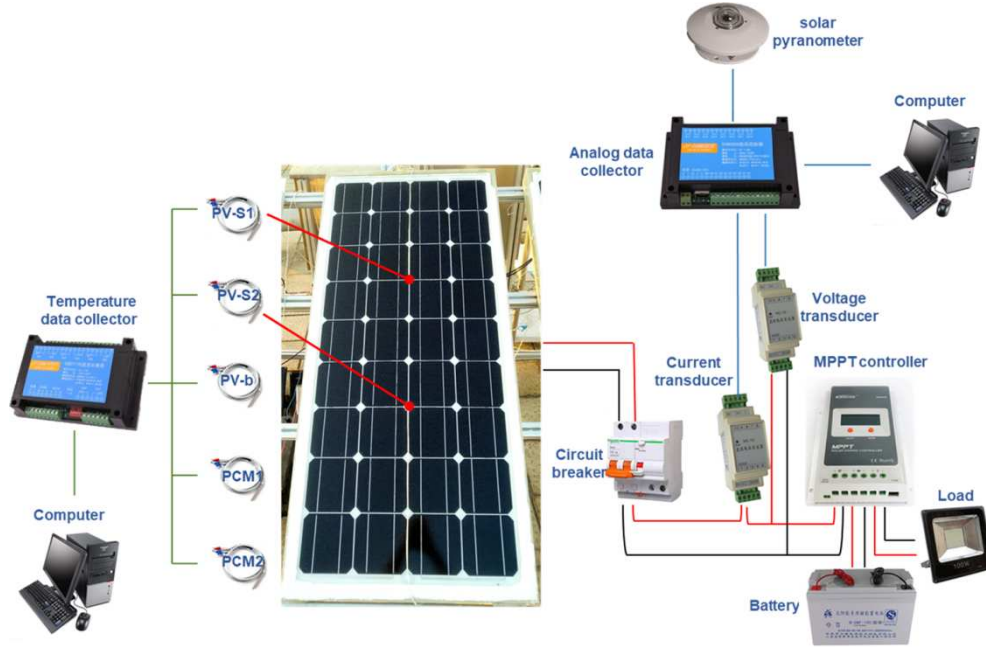### 4. Evaluating the effectiveness of PCM to reduce PV temperature

Fig. 11: Experimental design of PV-PCM system [79]

Table 6: The main terms for evaluation of PCMs effectiveness[16]

Description	Definition of parameter	No.
Peak temperature of the PV panel without PCM (℃)	$T_{peak-PV}$	-
Temperature of a PV-PCM panel at peak time (℃)	T_{PV-PCM}	-
Difference temperature (℃)	$\Delta T_{PV-peak} = T_{peak-PV} - T_{PV-PCM}$	(60)
Specific Mass of PCM (m_{spec}) in (kg m^{-2})	$m_{spec} = \dfrac{m_{PCM}}{A_{PV}}$	(61)
The required amount of PCM is determined by this parameter for one-meter square of the PV area		
The effective mass coefficient (m_{eff})in (kg m^{-2}℃$^{-1}$)	$m_{eff} = \dfrac{m_{spec}}{\Delta T_{PV-peak}}$	(62)
It is used to indicate how muchm_{spec}must be used to decrease one-degree peak PV temperature.		
Hasan et al. [66] proposed Eq. (63) for calculation of PV temperature at winter days.	$T_{PV} = T_{amb}\left(\dfrac{0.32}{8.91 + 2u_{wind}}\right)G$	(63)

Also, the performance of the PV-PCM systems can be calculated by the indicators shown in Table 7.

Table 7: Indicators to evaluate the performance of PV-PCM systems

Description	Definition of parameter	No.
The electrical efficiency is one of the major indicators [20, 44-46].	$\eta_{PV} = \eta_{ref}\left(1 - \beta_{cell}\left(T_{cell} - T_{ref}\right)\right)$	(64)
The power enhancement percentage (PEP)	$PEP = \dfrac{P_{out\_PCM} - P_{out\_ref}}{P_{out\_ref}} \times 100\%$	(65)
P_{out_PCM} and P_{out_ref} are the output power of the PV panels with and without PCM, , respectively [114].		
The efficiency enhancement percentage (EEP)	$EEP = \dfrac{\eta_{out\_PCM} - \eta_{out\_ref}}{\eta_{out\_ref}} \times 100\%$	(66)
η_{out_PCM} and η_{out_ref} are the efficiency of the PV panels with and without PCM, respectively [114].		
η is the energy efficiency	$\eta = \dfrac{P_s}{P_{e\_ref}}$	(67)
P_s is the energy savings (Wh) due to the integration of PCM.	where	
P_e is the electric power of the PV panel measured at$V_{oc}$and I_{sc} . FF is the fill factor and usually it is between 0.72 and 0.75. [66, 115].	$P_s = P_{e\_PV\_PCM} - P_{e\_ref}$	
	$P_e = \dfrac{V_{oc}I_{sc}}{FF}$	

The enhancement of thermal performance for a PV-PCM system [116].

$$Enhancment(\%) = \frac{T_{PV} - T_{PV-PCM}}{T_{PV}} \times 100\% \tag{68}$$

The total thermal regulation enhancement (Γ)[16, 17].

$$\Gamma = \sum_{t=0}^{t=n}\left(T_{PV,t} - T_{PV-PCM,t}\right) \tag{69}$$

In order to use PV-PCM systems, some questions must be answered which are summarized in Table 8. The second column of this table shows the answers to the questions that were obtained after the investigation.

Table 8: Main questions about PV-PCM systems

Main questions [16]	Answering into questions
1. What is a PV-PCM technology?	See subsection 1.3 and section 2
2. How much PV panel temperature can be reduced by using PCM?	PV panel temperature up to 20 °C and electrical efficiency up to 5% can be reduced by PCM[16].
3. How much mass of PCM is required to reduce temperature of the PV panel?	m_{eff} is approximately equal to 2.6 kg m^{-2}°C^{-1} (See Eq. 62) [16]
4. What must be the PCM melting point (T_m)for PV cooling application?	the selection of T_m depends on the climatic conditions and the geographical location Conventionally, $25°C < T_m < 35°C$ For the hot climatic conditions, $T_m > 35°C$. When PV temperature rises up to 90 °C, $T_{m,max} = 42°C$[16].
5. Which type of PCM (organic or inorganic) should be used?	In general, organic PCMs are more desirable, but inorganic PCMs have economic advantages. Also, see section 4 and Ref. [16].
6. Can the heat collected by PCM be used more or not?	See sections 5 (hybrid systems)
7. What problems might arise for PV-PCM systems?	The overall weight of PV panels increases if a large amount of PCM is used which leads to difficulty in installation.
8. What is the method of integrating PCM with PV panel?	See sections 2 and 5
9. Is PV-PCM technologically–economically feasible or not?	PV-PCM systems are suitable for the locations with high solar radiation and high ambient temperature(See section 6). An economic viability of the PV-PCM system was discussed by Waqas et al. [16], Hasan et al. [66] and Radziemska et al. [117].

It is worth mentioning that an ideal PCM should have large thermal conductivity, non-toxic,non-corrosive,large latent heat, inexpensive and chemically stable [118].PCMs are generally divided into three main groups: organic compounds, inorganic compounds and eutectic mixtures. A comparative merits and demerits of organic PCM, inorganic PCM and eutectics, can be found in the work of Islam et al.   [2].The performance of the inorganic and organic PCMs for cooling of PV panel were compared with each other by Hasan et al. [17]. Classification of the PCMs are given in Table 9.

Table 9: Classification of PCMs

Basis of classification	PCM denomination
Major capsulation techniques[16]	1. Macro-capsulated PCMs (capsulation size > 1 mm) 2. Micro-capsulated PCMs (1 µm <capsulation size <100 µm)
	Note: Macro-capsulation of PCM is cheaper than micro-capsulation
. Nature of PCM [17, 56]	1. Organic (such as RT20) Organic PCMs have lower thermal conductivity($0.1 < k < 0.2$ Wm^{-1}K^{-1}). 2. Inorganic (such as CaCl$_2$·6H$_2$O and Sp22) Inorganic PCMs have high thermal conductivity. 3. Eutectic mixtures (such as Capric–palmitic acid)
	Note: The use of inorganic PCMs is limited due to their corrosive nature and sub-cooling.

5.   Hybrid PV systems

Another area of PV-PCM research is the application of PCM to other types of PV systems, for example, PV/thermal (PV/T) system, concentrated PV (CPV) system,

and photovoltaic-thermoelectric (PV/TE) system [78].

5.1. Hybrid photovoltaic thermal (PVT) system

As mentioned before (see Fig. 1), the main applications of solar energy can be divided into two categories: solar thermal system and PV system. Usually, these systems are applied separately. In the solar thermal system, external electrical energy is required for the circulation of the working fluid in the system. On the other hand, in the PV system, the electrical efficiency of the system decreases rapidly when the temperature of PV module increases. Therefore, the scientists proposed hybrid photovoltaic-thermal collectors (PV/T)which generate electric power and

simultaneous produce hot airor hot water[108]. Besides the higher overall energy performance, the advantage of the PV/T collector system lies in reducing the need for physical space and the cost of equipment[119].In order to evaluate the performance of a PV/T collector, the amount of electricity compared to the useful heat from the collector is a main factor. The performance of a PVT collector can also be assessed in terms of exergy efficiency [120]. Sarhaddi et al. [119]reviewed the literature for PVT exergy efficiency. Also, Fig. 12 represents the cross-sectional view of a PV/T air collector and thermal resistance modeling [119].
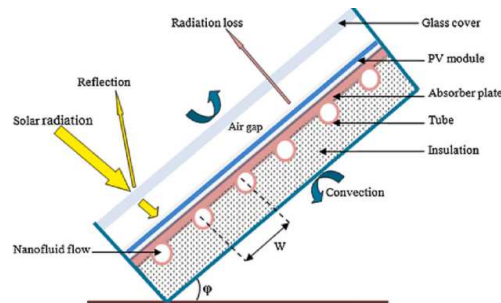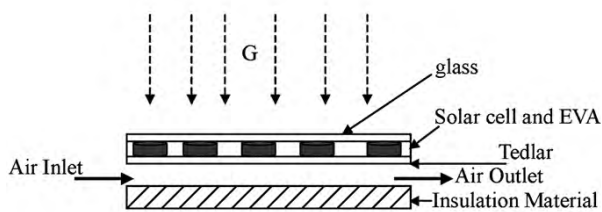

Fig. 12: (a) The cross-sectional view of a PV/T air collector[119], (b) Schematic of a PVT systems [121]

5.2. Hybrid photovoltaic-thermoelectric (PV/TE) system

As we know, the thermoelectric (TE) technology can directly convert heat into electricity due to the Seebeck effect. A combination of photovoltaic (PV) and thermoelectric (TE), known as the photovoltaic-thermoelectric (PV-TE) hybrid system, is an effective way to increase the total power output [122]. Fig. 13 represents

an example of the structural diagram of the PV and PV-TE systems. Also, the energy transfer networks of PV and PV-TE system based on thermal resistance model are presented in Fig. 14. As shown, both networks are similar to each other, including boundary condition, except for the other two thermal resistances, TEG and gel. For more details, one can refer to work of Gu et al. [122].
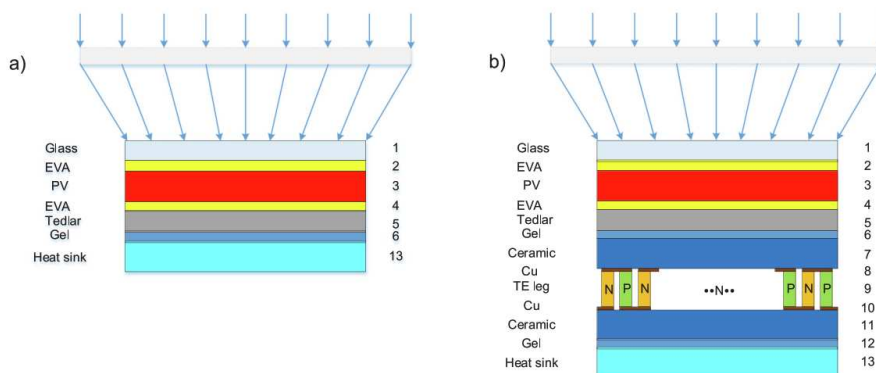

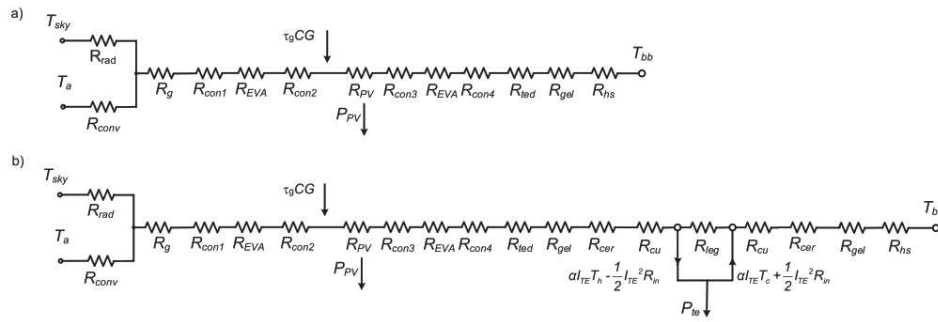**Fig. 13:** Structural diagram of the two systems: (a) PV; (b) PV-TE. [122]

Fig. 14: Schematic diagram of energy transfer networks: (a) PV; (b) PV-TE. [122]

5.3. Hybrid photovoltaic-PCM-thermoelectric (PV-PCM-TE) system

The integration of PCM systems and PV-TE hybrid system can be an effective way to cool the PV panel and increase the power generation. The PV-PCM-TE system consists of a PVcell, shape-stabilized PCM plate and TE module. As shown in Fig. 15the solar radiation is absorbed by the PV cell while the PCM is deployed between the TE modules and the PV cell. During operation, the solar energy is imposed on the PV modules, then the thermal energy is transferred to the upper surface of the PCM, the energy is absorbed by the PCM or transferred to the connected TE modules. The mathematical model of the PV-PCM-TE system can be found in the study of Luo et al. [123].
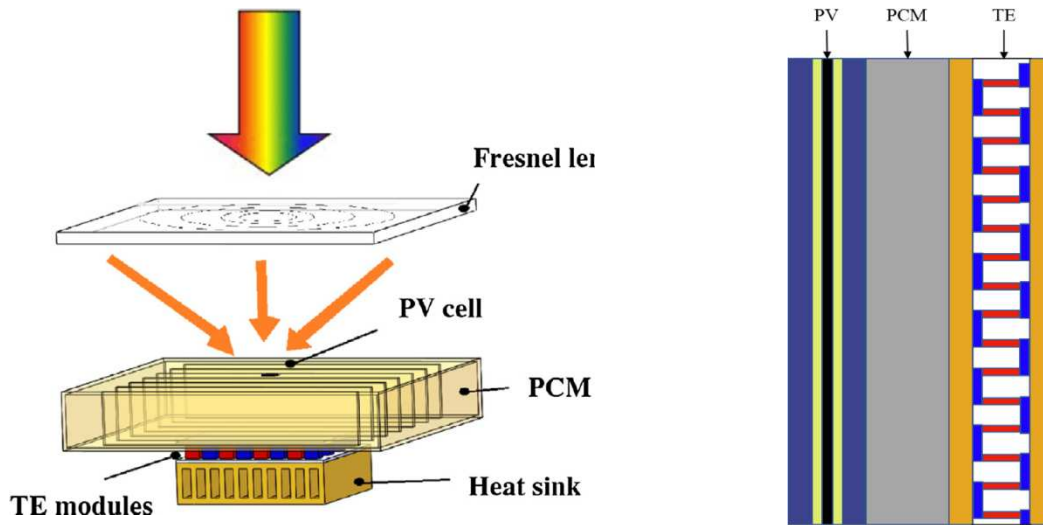
Fig. 15:(a) PV-TE-PCM hybrid system schematic [2], (b) The geometrical structure of the PV-PCM-TE system [123]

6. Economic feasibility of PV-PCM systems

Radziemska [117]performed an economic analysis for a PV-PCM system. They found that the cost of modified PV-PCM system (1 kW_p capacity) can be 8.5% higher than the cost of a simple PV. Of course it produces 7% more energy for each year. In another work, Hasan et al. [66] observed that a PV-PCM system can produce 13.5 kWh/m^2 of additional energy to compared to a simple PV. Therefore, it provides an economic benefit of 2.02 $/m^2$ (13.5 kWh/m^2 × 0.15 $/kWh = 2.02$/m^2$). The cost of electricity is assumed to be 0.15 $/kWh. Here, 27 kg of PCM was used for onem^2 of PV area. The cost of paraffin wax (organic PCM) and slat hydrates (inorganic PCMs) is 1.0 $/kg and 0.14–0.24 $/kg, respectively. Therefore, they can produce a payback within 10–12 years and 3-4 years, respectively. Table 10 represents a summary of the major works on the different PV systems.

Table 10: Some major works on the different PV systems

Literature	Type of system
[4], [7], [9-14], [42,43], [70], [76], [86-88], [90-94], [103,104], [108], [124-145]	PV system
[15-20], [44-46], [53-58], [60-68], [71-82], [105], [107], [113-118], [146,147]	PV-PCM system
[84], [122], [148,149]	PV-TE system
[123], [150-153]	PV-PCM-TE system
[56], [69], [119-121], [154]	PVT or CPVT system

7. Investigation the effect of active parameters on the PV-PCM system

In this section the effect of main parameters on the performance of PV or PV-PCM systems is reviewed. On the other word, the main outcomes of the literature, are summarized in below.

7.1. Output power and current versus voltage in a PV cell

As mentioned before, in 2021, Sharfabadi et al.[87] investigated the energy and exergy analysis of 190 W PV cell. Table 11 represents the characteristics of PV cell at reference conditions. A code in the equation engineering solver (EES) software was extended to recalculate the original results. The outcomes are presented in the Figs. 16-18.

Table 11: The characteristics of solar cell at reference conditions[87]

Parameters	Value
Maximum power , P_{mp}(W)	191.861
open circuit voltage, V_{oc}(V)	44.988
short circuit current, I_{sc}(A)	5.733
maximum power point voltage, V_{mp}(V)	36.055
maximum power point current, I_{mp}(A)	5.321
Shunt resistance, R_{sh}(Ω)	388.485
series resistance of cell, R_s(Ω)	0.982
The voltage temperature coefficient μ_{oc}(V/K)	-0.0033
The current temperature	0.0003

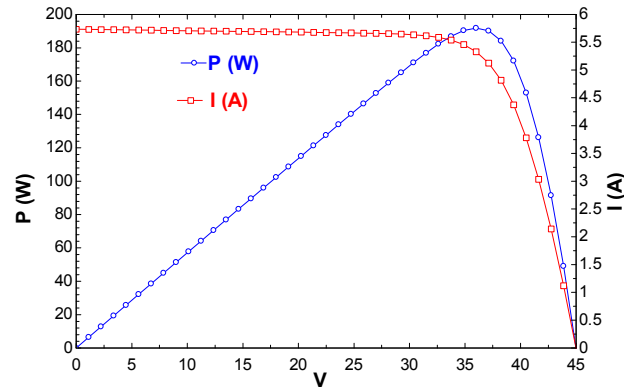| coefficient, μ_{sc}(A/K)	
Number of cells N	72 (6 × 12)
Dimensions (mm)	1580 × 808 × 45

Fig. 16: Output power and current versus voltage at reference conditions(recalculated from Ref. [87])
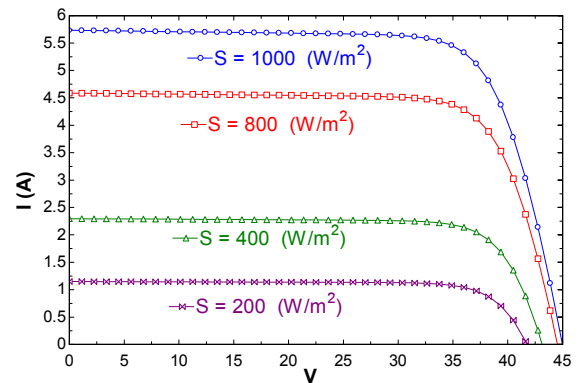

Fig. 17: Current versus voltage at different values of solar intensity (recalculated from Ref. [87])
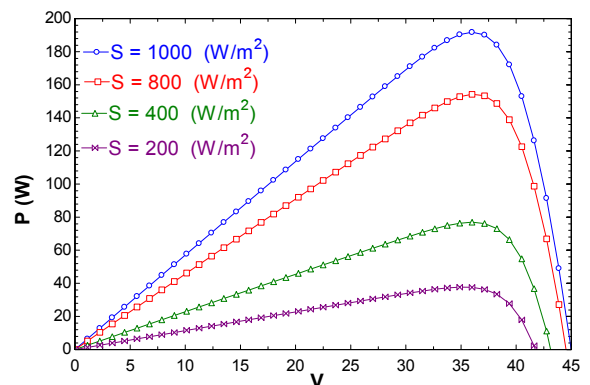

Fig. 18: Output power versus voltage at different values of solar intensity (recalculated from Ref. [87])

7.2. Analysis of a PV system

Note: At the beginning, it should be stated that, the Figs. 19-23are borrowed from Sánchez Barroso's article[86].

➤ The *I–V* and *P–V* curves

The *I–V* curve of the PV panel can be plotted using the values of the shunt and series resistances.   The *I–V* and *P–*

V curves for the PV panel BP 350 at Standard Test Conditions (STC) were plotted by Siddiquiet al. [88] and Tsai [89]that are shown in Fig. 19 [86].
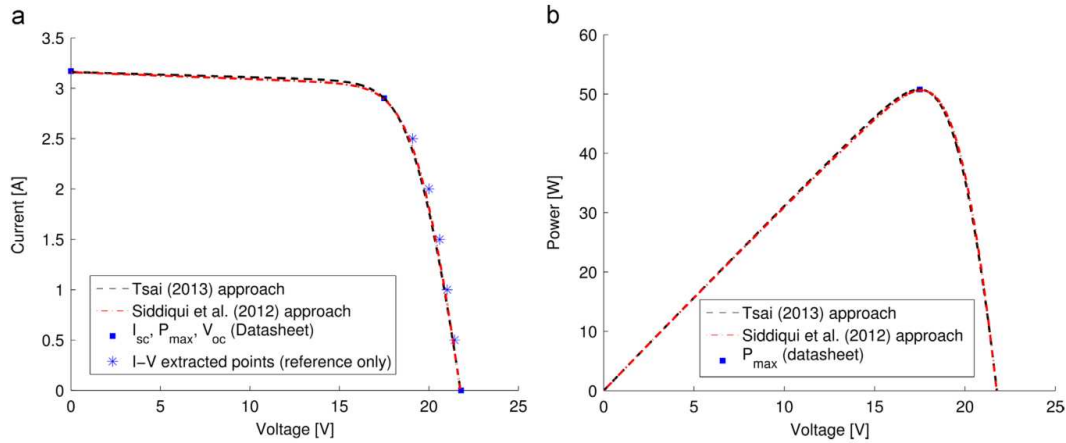
Fig. 19: Curves for the PV panel BP 350 at STC calculated by Siddiqui et al. [88] and Tsai [89]: (a) I–V curves, (b) P–V curves

➤ The effects of cell temperature and global solar radiation on the *I–V* curve

The curves for three different temperatures at constant solar irradiance are shown in Fig. 20a. Also, the curves for

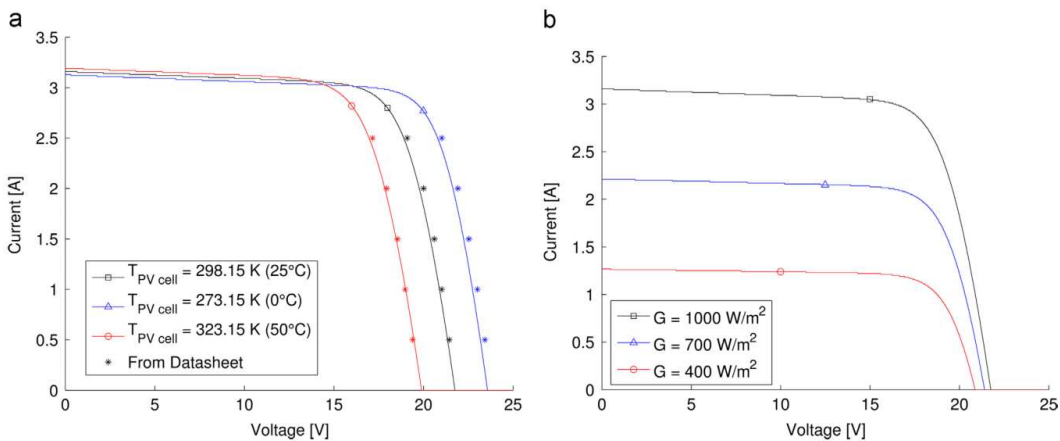three different global solar radiations at constant cell temperature are shown in Fig. 20b. [86]

Fig. 20: I–V curves for a Panel BP 350at: (a) different cell temperatures and (b) different global solar radiations.

➤ The effects of ambient temperature, global solar radiation and wind speed on the PV cell temperature

The effects of ambient temperature, global solar radiation and wind speed on the PV cell temperature are shown in Figs. 21-23.This figure discovers that there is a certain wind speed (near or above 1 m/s) which the temperature of the cells decreases.
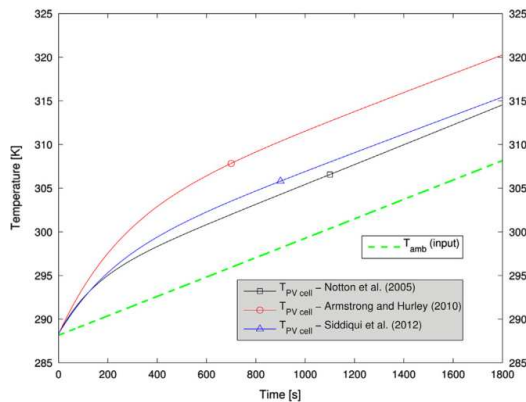
Fig. 21:PV cell temperatures with changing ambient temperature [86]
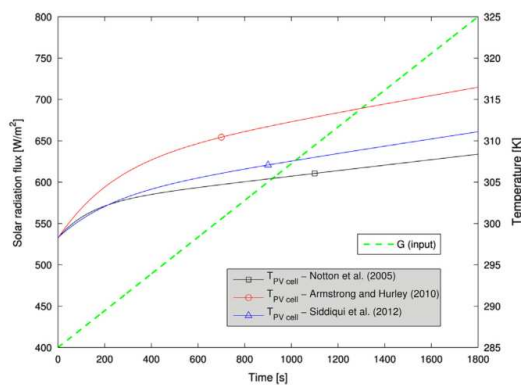

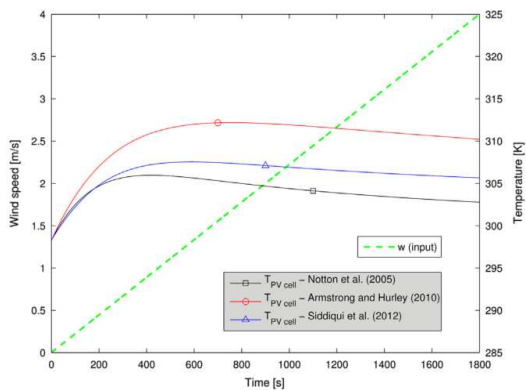**Fig. 22:**PV cell temperatures with changing global solar radiation[86]

Fig. 23: PV cell temperatures with changing wind speed[86]

7.3. Analysis of a PV-PCM system

As mentioned before, in 2018, the mathematical modelling of a PV-PCM was performed by Ma et al. [78]. Fig. 24 represents a comparison between the PV temperature profile modelled by the thermal resistance method (MATLAB program) and CFD method (FLUENT program). Fig. 25 represents a sample result of CFD modelling. Liquid fraction and temperature distributions can be seen in

this figure. Figs. 24 and 25are corresponding to Table 2 and Figs. 4, 9and 10. Figs. 24 and 25 were taken from Ref. [78].
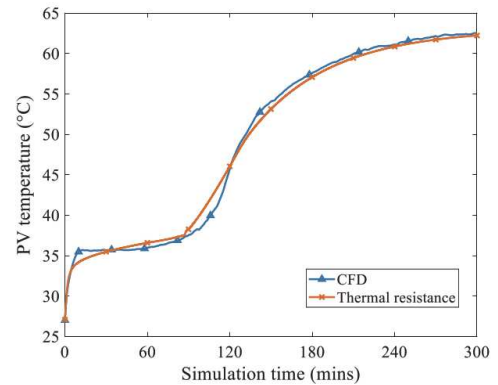

Fig. 24: PV temperature profile modelled by thermal resistance method (MATLAB program) and CFD method (FLUENT program)[78]
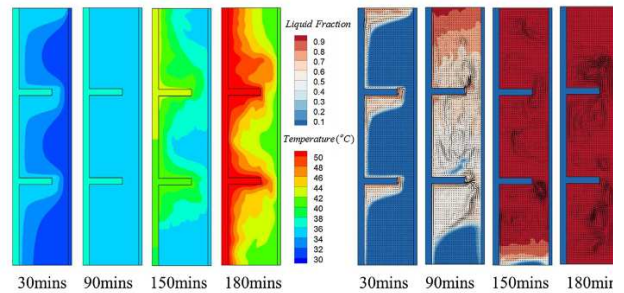

Fig. 25: The CFD simulation result of a PV-PCM system[78]

7.4. Experimental Analysis of a PV-PCM system

In 2019, Zhao et al. [79] investigated a PV-PCM system theoretically and experimentally. Fig. 26 shows a comparison between the simulation result and the experimental data (for a summer day of Shanghai). Fig. 26 is corresponding to Figs. 8and 11.
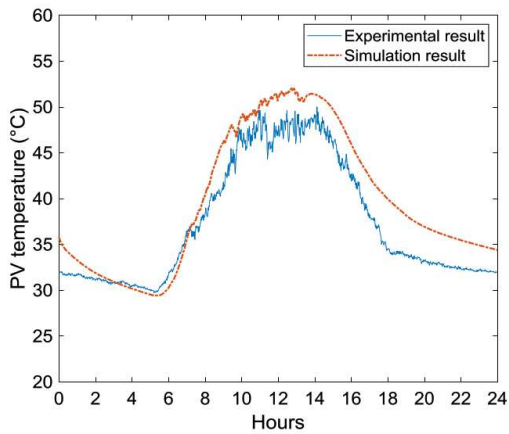
Fig. 26: PV temperature including the experimental data and the simulation result [79].
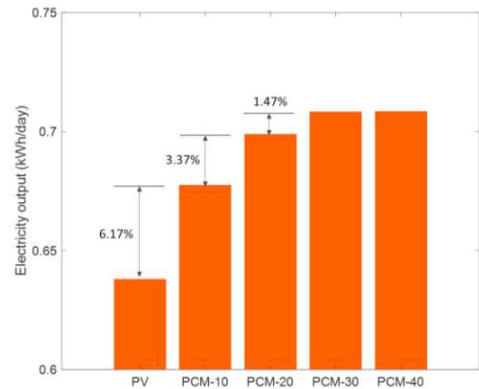
7.5. Effect of PCM thickness on the performance of a PV-PCM system

Performance analysis of a PV panel integrated with PCM was investigated by Zhao et al. [155]. Comparison of PV temperature between PV-only system and PV-PCM system (30 mm PCM) is shown in Fig. 27. Also, Fig. 28 shows the output power of system for different values of PCM thickness. The simulation result discovers that the PV temperature can be reduced by about 25°C using PCM and thus the electricity output can be increased by approximately 11%. [155].

Fig. 27: PV temperature for PV-onlyand PV-PCM system (30 mm PCM) [155]

Fig. 28: Electricity output of PV-PCM system for different values of PCM thickness [155]

7.6. Analysis of a PV-TE system

As mentioned before, in 2019, Gu et al. [122]evaluated performance of a hybrid photovoltaic-thermoelectric system. PV-TE system. The Figs. 29-32 are borrowed from this paper. Fig. 29 presents the PV cell temperature that has been calculated by CFD analysis (Ansys software) and the thermal resistance model (MATLAB code). Fig. 30represents the efficiency versus concentration ratio for PV and PV-TE systems. The variations of power, efficiency and temperature for PV and PV-TE systems in a sunny day are shown in Figs. 31 and 32.
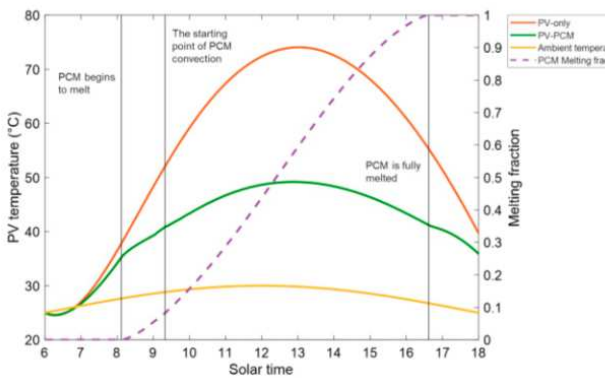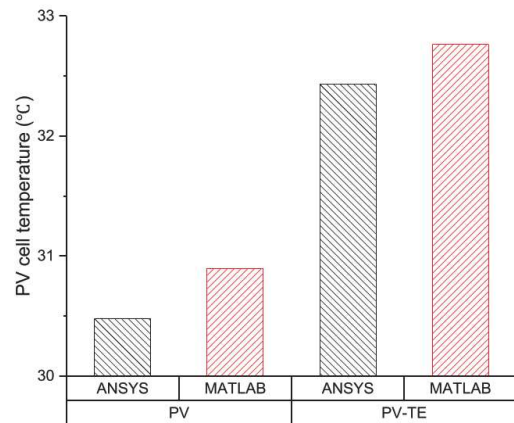

Fig. 29: Validation of PV and PV-TE model [122]
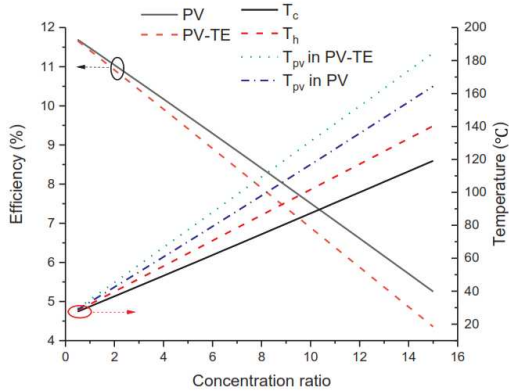
Fig. 30: The efficiency versus concentration ratio [122]
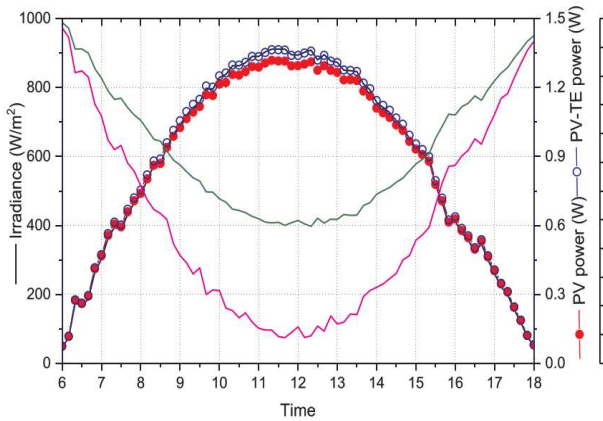
Fig. 31: The power and efficiency of PV and PV-TE under a sunny case [122]
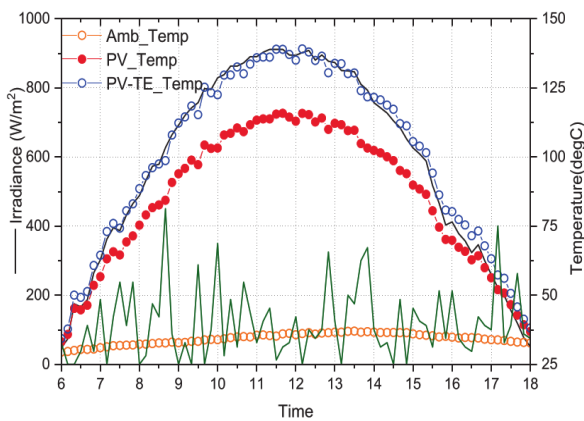
Fig. 32: The temperature variation under sunny case[122]

7.7.Analysis of a PV-PCM-TE system

As mentioned earlier, in 2022, Luo et al. [123] studied the performance of a PV-PCM-TE system during the year. The meteorological parameters in summer has been given in Fig. 33. Figs. 34 and 35 represent the solar cell temperature of PV and its output power. Also, Fig. 36 shows the electrical efficiency and annual total electrical power for

three systems (PV, PV-TE and PV-PCM-TE systems). The results show that the last system (PV-PCM-TE) is the most favorable.
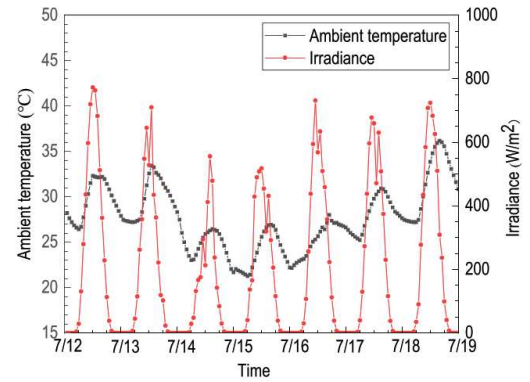
Fig. 33: The meteorological parameters in summer [123]
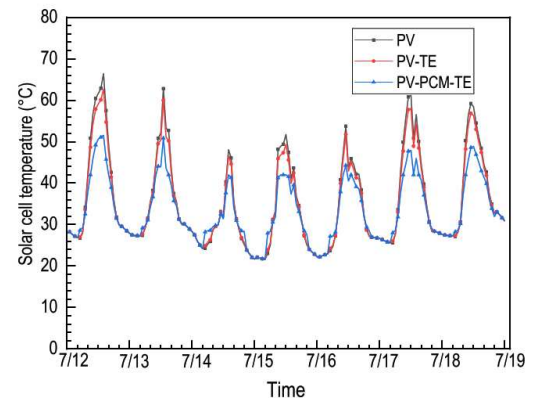
Fig. 34: Solar cell temperature of PV in summer [123]
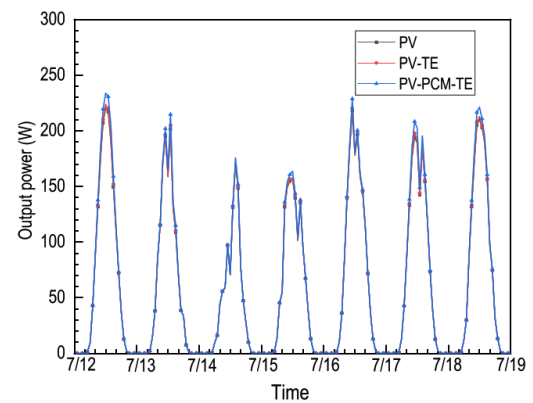
Fig. 35: Output power of PV in summer [123]

Fig. 36: Electrical efficiency and annual total electrical power for three systems [123]

8. Future developments

The continuous reduction in the cost of PV arrays and increasing their efficiency have a promising role for PV generation systems in the near future. The life of solar cells increases using cooling techniques because these methods lead to the reduction of thermal stresses. Investigations on the possibility of using PCMs as a medium of thermal regulation in PV systems is now a growing field of research all over the globe. It should be noted that PV-PCM systems are not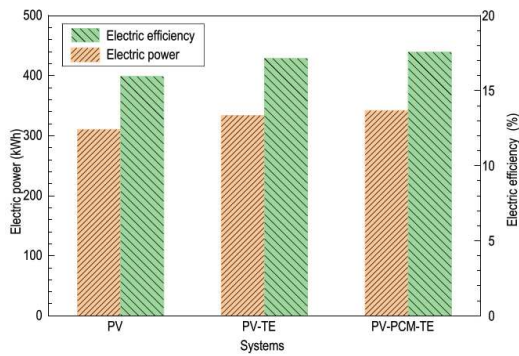 yet commercialized because of high system cost, technological challenges and availability of appropriate PCMs. However, PV-PCM systems are still in the research

stage and have a wide scope for practical applications. Suggestions for the future works were provided by Waqas et al. [16]. Rea et al. [156] stated that CPV integrated with PCM is a promising and practical application of PV-PCM system in the near future.

9. Summary

In the present study, firstly, conventional PV system integrated with PCM (known as PV-PCM) was critically reviewed. Then, after explaining the PV-PCM system configuration, mathematical modeling including electrical model, solar radiation model and electricity generation model was presented. The improved 1-D thermal resistant model (the enhanced conductivity method) was explained. Indicators to access the performance of PV-PCM systems were presented. Hybrid systems including PVT, PV-TE, and PV-PCM-TE were presented. The effects of main parameters on the performance of PV or PV-PCM systems were investigated. It has been observed that PCM can effectively reduce the operating temperature of the PV panel and improve electrical efficiency of the PV panels. Table 12 summarized the advantages and disadvantages of PV-PCM systems.

Table 12: The advantages and disadvantages of PV-PCM systems

Advantages	Disadvantages
Temperature reduction of PV panels	Uneconomic
	Unavailability of optimal PCMs
Energy storage	Lack of proper disposal technology for used PCM after completion of their life cycle
Saving energy	
High heat absorption rate	
No moving parts	
No electricity consumption	
No maintenance cost	

Nomenclature

a	Modified diode ideality factor (eV)	G_b	Direct (beam) solar radiations (Wm^{-2})
A	Area (m^2)	G_d	Diffuse solar radiations (Wm^{-2})
C_p	Specific heat $(J\,kg^{-1}K^{-1})$	Gr	Grashof number $(-)$
EEP	Efficiency enhancement percentage (%)	h	Heat transfer coefficient $(W\,m^{-2}K^{-1})$
Ex	Exergy (W)	I	Circuit current (A)
F	View factor	$I_{C.V}$	Irreversibility in control volume (J)
FF	Fill Factor	k	Thermal conductivity $(W\,m^{-1}K^{-1})$
G	Solar radiation intensity $(W\,m^{-2})$	k_B	Boltzmann constant (JK^{-1})
		L	Length of solar module (m)
		m_{spec}	Specific Mass of PCM $(kg\,m^{-2})$

m_{eff}	Effective mass coefficient $(\mathrm{kg\,m^{-2}{}^{\circ}C^{-1}})$		O	Open-circuit
N_s	Number of PV cells connected in series		c	
N_p	Number of PV cells connected in parallel		R	Reference
P	Power output (W)		ef	
P	Phase change material		S	Series
CM			S	Shunt
Pr	Prandtl number $(-)$		h	
PV	Photovoltaic			
PV/T	Photovoltaic/Thermal collector			
q_e	Electron charge (C)			
R	Resistance (Ω)			
Ra	Rayleigh number $(-)$			
S	solar absorbed flux (W)			
T	Temperature (K)			
T_c	Operating temperature (K)			
T	Thermoelectric			
E				
u_{wind}	Wind velocity $(\mathrm{ms^{-1}})$			
V	Circuit voltage (V)			
W	Width of solar module (m)			
Y_{cell}	Solar radiation coefficient $(-)$			
	Greek Symbols			
α_n	Diode ideality factor $(-)$			
β	Tilt angle of the PV panel $(°)$			
β_{cell}	Temperature coefficient of the PV cell			
ε	Emissivity $(-)$			
η_{el}	Electrical efficiency $(-)$			
μ_{oc}	Voltage temperature coefficient $(\mathrm{VK^{-1}})$			
μ_{sc}	Current temperature coefficient $(\mathrm{AK^{-1}})$			
ρ	density of the material of the layer $(\mathrm{kg\,m^{-3}})$			
σ	Stefan-Boltzmann's constant $(\mathrm{W\,m^{-2}K^{-4}})$			
$(\tau\alpha)$	The effective product oftransmittance-absorptance			
φ	Latitude of the location			
Γ	Total thermal regulation enhancement $(-)$			
	Subscripts			
a	Ambient			
mb				
d	Destruction			
est				
M	Module			
od				
M	Maximum power point			
p				

References

[1] Seyyedi SM. Thermoeconomic Analysis of a Steam Rankine Cycle Integrated with Parabolic Trough Solar Collectors. Journal of Applied Dynamic Systems and Control. 2021 Jun 1;4(1):1-7.

[2] Islam MM, Pandey AK, Hasanuzzaman M, Rahim NA. Recent progresses and achievements in photovoltaic-phase change material technology: A review with special treatment on photovoltaic thermal-phase change material systems. Energy Conversion and Management. 2016 Oct 15;126:177-204.

[3] Seyyedi SM, Hashemi-Tilehnoee M, Sharifpur M. Thermoeconomic analysis of a solar-driven hydrogen production system with proton exchange membrane water electrolysis unit. Thermal Science and Engineering Progress. 2022 May 1;30:101274

[4] Ma T, Yang H, Lu L. Solar photovoltaic system modeling and performance prediction. Renewable and Sustainable Energy Reviews. 2014 Aug 1;36:304-15.

[5] Enslin JH. Maximum power point tracking: a cost saving necessity in solar energy systems. In[Proceedings] IECON'90: 16th Annual Conference of IEEE Industrial Electronics Society 1990 Nov 27 (pp. 1073-1077). IEEE.

[6] van Helden WG, van Zolingen RJ, Zondag HA. PV thermal systems: PV panels supplying renewable electricity and heat. Progress in photovoltaics: research and applications. 2004 Sep;12(6):415-26.

[7] Singh GK. Solar power generation by PV (photovoltaic) technology: A review. Energy. 2013 May 1;53:1-3.

[8] Zweibel Kenneth, Herch Paul. Basic photovoltaic principles and methods. New York: Van Nosstrand Reinhold Company, Inc.; 1984.

[9] Ma T, Yang H, Lu L. Development of a model to simulate the performance characteristics of crystalline silicon photovoltaic modules/strings/arrays. Solar Energy. 2014 Feb 1;100:31-41.

[10] Tian Y, Zhao CY. A review of solar collectors and thermal energy storage in solar thermal applications. Applied energy. 2013 Apr 1;104:538-53.

[11] Skoplaki E, Palyvos JA. On the temperature dependence of photovoltaic module electrical performance: A review of efficiency/power correlations. Solar energy. 2009 May 1;83(5):614-24.

[12] Ma T, Yang H, Lu L. Performance evaluation of a stand-alone photovoltaic system on an isolated island in Hong Kong.

Applied Energy. 2013 Dec 1;112:663-72.

[13] Armstrong S, Hurley WG. A thermal model for photovoltaic panels under varying atmospheric conditions. Applied thermal engineering. 2010 Aug 1;30(11-12):1488-95.

[14] Jones AD, Underwood CP. A thermal model for photovoltaic systems. Solar energy. 2001 Jan 1;70(4):349-59.

[15] Browne MC, Norton B, McCormack SJ. Phase change materials for photovoltaic thermal management. Renewable and Sustainable Energy Reviews. 2015 Jul 1;47:762-82.

[16] Waqas A, Ji J, Xu L, Ali M, Alvi J. Thermal and electrical management of photovoltaic panels using phase change materials– A review. Renewable and Sustainable Energy Reviews. 2018 Sep 1;92:254-71.

[17] Hasan A, McCormack SJ, Huang MJ, Norton B. Evaluation of phase change materials for thermal regulation enhancement of building integrated photovoltaics. Solar Energy. 2010 Sep 1;84(9):1601-12.

[18] Siecker J, Kusakana K, Numbi EB. A review of solar photovoltaic systems cooling technologies. Renewable and Sustainable Energy Reviews. 2017 Nov 1;79:192-203.

[19] Kenisarin M, Mahkamov K. Solar energy storage using phase change materials. Renewable and sustainable energy reviews. 2007 Dec 1;11(9):1913-65.

[20] Atkin P, Farid MM. Improving the efficiency of photovoltaic cells using PCM infused graphite and aluminium fins. Solar Energy. 2015 Apr 1;114:217-28.

[21] Ling Z, Zhang Z, Shi G, Fang X, Wang L, Gao X, Fang Y, Xu T, Wang S, Liu X. Review on thermal management systems using phase change materials for electronic components, Li-ion batteries and photovoltaic modules. Renewable and Sustainable Energy Reviews. 2014 Mar 1;31:427-38.

[22] Gharbi S, Harmand S, Jabrallah SB. Experimental comparison between different configurations of PCM based heat sinks for cooling electronic components. Applied Thermal Engineering. 2015 Aug 5;87:454-62.

[23] Shalaby SM, Bek MA, El-Sebaii AA. Solar dryers with PCM as energy storage medium: A review. Renewable and Sustainable Energy Reviews. 2014 May 1;33:110-116.

[24] Agyenim F. The use of enhanced heat transfer phase change materials (PCM) to improve the coefficient of performance (COP) of solar powered LiBr/H2O absorption cooling systems. Renewable Energy. 2016 Mar 1;87:229-39.

[25] Maruoka N, Akiyama T. Thermal stress analysis of PCM encapsulation for heat recovery of high temperature waste heat. Journal of chemical engineering of Japan. 2003;36(7):794-8.

[26]Nomura T, Okinaka N, Akiyama T. Waste heat transportation system, using phase change material (PCM) from steelworks to chemical plant. Resources, Conservation and Recycling. 2010 Sep 1;54(11):1000-6.

[27] Tiari S, Qiu S, Mahdavi M. Numerical study of finned heat pipe-assisted thermal energy storage system with high temperature phase change material. Energy Conversion and Management. 2015 Jan 1;89:833-42.

[28] Tiari S, Qiu S, Mahdavi M. Discharging process of a finned heat pipe–assisted thermal energy storage system with high temperature phase change material. Energy Conversion and Management. 2016 Jun 15;118:426-37.

[29] Ghalambaz M, Chamkha AJ, Wen D. Natural convective flow and heat transfer of nano-encapsulated phase change materials (NEPCMs) in a cavity. International journal of heat and mass transfer. 2019 Aug 1;138:738-49.

[30] Leong KY, Saidur R, Kazi SN, Mamun AH. Performance investigation of an automotive car radiator operated with nanofluid-based coolants (nanofluid as a coolant in a radiator). Applied Thermal Engineering. 2010 Dec 1;30(17-18):2685-92.

[31] Saidur R, Leong KY, Mohammed HA. A review on applications and challenges of nanofluids. Renewable and sustainable energy reviews. 2011 Apr 1;15(3):1646-68.

[32] Yousefi T, Veysi F, Shojaeizadeh E, Zinadini S. An experimental investigation on the effect of Al2O3–H2O nanofluid on the efficiency of flat-plate solar collectors. Renewable Energy. 2012 Mar 1;39(1):293-8.

[33] Seyyedi SM, Hashemi-Tilehnoee M, Sharifpur M. Effect of inclined magnetic field on the entropy generation in an annulus filled with NEPCM suspension. Mathematical Problems in Engineering. 2021 Aug 14;2021:1-4.

[34] Mansour MA, Bakier MA. Free convection heat transfer in complex-wavy-wall enclosed cavity filled with nanofluid. International Communications in Heat and Mass Transfer. 2013 May 1;44:108-15.

[35] Dogonchi AS, Waqas M, Seyyedi SM, Hashemi-Tilehnoee M, Ganji DD. CVFEM analysis for Fe3O4–H2O nanofluid in an annulus subject to thermal radiation. International Journal of Heat and Mass Transfer. 2019 Apr 1;132:473-83.

[36] Seyyedi SM, Dogonchi AS, Hashemi-Tilehnoee M, Waqas M, Ganji DD. Entropy generation and economic analyses in a nanofluid filled L-shaped enclosure subjected to an oriented magnetic field. Applied Thermal Engineering. 2020 Mar 5;168:114789.

[37] Hashemi-Tilehnoee M, Tashakor S, Dogonchi AS, Seyyedi SM, Khaleghi M. Entropy generation in concentric annuli of 400 kV gas-insulated transmission line. Thermal Science and Engineering Progress. 2020 Oct 1;19:100614.

[38] Seyyedi SM, Dogonchi AS, Hashemi-Tilehnoee M, Ganji DD, Chamkha AJ. Second law analysis of magneto-natural convection in a nanofluid filled wavy-hexagonal porous enclosure. International Journal of Numerical Methods for Heat & Fluid Flow. 2020 Oct 15;30(11):4811-36.

[39] Hashemi-Tilehnoee M, Dogonchi AS, Seyyedi SM, Chamkha AJ, Ganji DD. Magnetohydrodynamic natural convection and entropy generation analyses inside a nanofluid-filled incinerator-shaped porous cavity with wavy heater block. Journal of Thermal Analysis and Calorimetry. 2020 Sep;141(5):2033-45.

[40] Seyyedi SM, Hashemi-Tilehnoee M, Palomo del Barrio E, Dogonchi AS, Ghadami SM, Sharifpur M. Electro-enhanced natural convection analysis for an Al2O3-water-filled enclosure by considering the effect of thermal radiation. Numerical Heat Transfer, Part A: Applications. 2023 Aug 2:1-20.

[41] Seyyedi SM. On the entropy generation for a porous enclosure subject to a magnetic field: different orientations of cardioid geometry. International Communications in Heat and Mass Transfer. 2020 Jul 1;116:104712.

[42] Elmir M, Mehdaoui R, Mojtabi A. Numerical simulation of cooling a solar cell by forced convection in the presence of a nanofluid. Energy Procedia. 2012 Jan 1;18:594-603.

[43] Cui Y, Zhu Q. Study of photovoltaic/thermal systems with MgO-water nanofluids flowing over silicon solar cells. In 2012 Asia-pacific power and energy engineering conference 2012 Mar 27 (pp. 1-4). IEEE.

[44] Ho CJ, Tanuwijava AO, Lai CM. Thermal and electrical performance of a BIPV integrated with a microencapsulated phase change material layer. Energy and Buildings. 2012 Jul 1;50:331-8.

[45] Ho CJ, Chou WL, Lai CM. Thermal and electrical performance of a water-surface floating PV integrated with a water-saturated MEPCM layer. Energy Conversion and Management. 2015 Jan 1;89:862-72.

[46] Tanuwijava AO, Ho CJ, Lai CM, Huang CY. Numerical investigation of the thermal management performance of MEPCM modules for PV applications. Energies. 2013 Aug 6;6(8):3922-36.

[47] Hajjar A, Mehryan SA, Ghalambaz M. Time periodic natural convection heat transfer in a nano-encapsulated phase-change suspension. International Journal of Mechanical Sciences. 2020 Jan 15;166:105243.

[48] Hashemi-Tilehnoee M, Dogonchi AS, Seyyedi SM, Sharifpur M. Magneto-fluid dynamic and second law analysis in a hot porous cavity filled by nanofluid and nano-encapsulated phase change material suspension with different layout of cooling channels. Journal of Energy Storage. 2020 Oct 1;31:101720.

[49] Hashem Zadeh SM, Mehryan SA, Sheremet M, Ghodrat M, Ghalambaz M. Thermo-hydrodynamic and entropy generation analysis of a dilute aqueous suspension enhanced with nano-encapsulated phase change material. International Journal of Mechanical Sciences. 2020 Jul 15;178:105609.

[50] Hashem Zadeh SM, Mehryan SA, Islam MS, Ghalambaz M. Irreversibility analysis of thermally driven flow of a water-based suspension with dispersed nano-sized capsules of phase change material. International Journal of Heat and Mass Transfer. 2020 Jul 1;155:119796.

[51] Seyyedi SM, Hashemi-Tilehnoee M, Sharifpur M. Impact of fusion temperature on hydrothermal features of flow within an annulus loaded with nanoencapsulated phase change materials (NEPCMs) during natural convection process. Mathematical Problems in Engineering. 2021 Nov 10;2021:1-14.

[52] Stultz JWWL. Thermal performance testing and analysis of photovoltaic modules in natural sunlight. Pasadena (California): Jet Propulsion Laboratory; 1978.

[53] Huang MJ, Eames PC, Norton B. Thermal regulation of building-integrated photovoltaics using phase change materials. International Journal of heat and mass transfer. 2004 Jun 1;47(12-13):2715-33.

[54] Huang MJ, Eames PC, Norton B. Phase change materials for limiting temperature rise in building integrated photovoltaics. Solar energy. 2006 Sep 1;80(9):1121-30.

[55] Stritih U. Increasing the efficiency of PV panel with the use of PCM. Renewable Energy. 2016 Nov 1;97:671-9.

[56] Browne MC, Norton B, McCormack SJ. Heat retention of a photovoltaic/thermal collector with PCM. Solar Energy. 2016 Aug 1;133:533-48.

[57] Hasan A, Alnoman H, Rashid Y. Impact of integrated photovoltaic-phase change material system on building energy efficiency in hot climate. Energy and Buildings. 2016 Oct 15;130:495-505.

[58] Huang MJ, Eames PC, Norton B. Comparison of predictions made using a new 3D phase change material thermal control model with experimental measurements and predictions made using a validated 2D model. Heat Transfer Engineering. 2007 Jan 1;28(1):31-7.

[59] Huang MJ, Eames PC, Norton B. Comparison of a small-scale 3D PCM thermal control model with a validated 2D PCM thermal control model. Solar energy materials and solar cells. 2006 Aug 15;90(13):1961-72.

[60] Huang MJ, Eames PC, Norton B, Hewitt NJ. Natural convection in an internally finned phase change material heat sink for the thermal management of photovoltaics. Solar Energy Materials and Solar Cells. 2011 Jul 1;95(7):1598-603.

[61] Nizetic, S., A. M. Papadopoulos, and E. Giama. 2017. Comprehensive analysis and general economic-environmental evaluation of cooling techniques for photovoltaic panels, part I: Passive cooling techniques. Energy Conversion and Management 149:334–54. doi:10.1016/j.enconman.2017.07.022.

[62] Nizetic, S., M. Jurcevic, D. Coko, and M. Arici. 2021. A novel and effective passive cooling strategy for photovoltaic panel. Renewable & Sustainable Energy Reviews 145. doi:10.1016/j.rser.2021.111164.

[63] Aneli S, Arena R, Gagliano A. Numerical Simulations of a PV Module with Phase Change Material (PV-PCM) under Variable Weather Conditions. International Journal of Heat & Technology. 2021 Apr 1;39(2).

[64] Hasan A, McCormack SJ, Huang MJ, Norton B. Energy and cost saving of a photovoltaic-phase change materials (PV-PCM) system through temperature regulation and performance enhancement of photovoltaics. Energies. 2014 Mar 5;7(3):1318-31.

[65] Park J, Kim T, Leigh SB. Application of a phase-change material to improve the electrical performance of vertical-

building-added photovoltaics considering the annual weather conditions. Solar Energy. 2014 Jul 1;105:561-74.

[66] Hasan A, Sarwar J, Alnoman H, Abdelbaqi ES. Yearly energy performance of a photovoltaic-phase change material (PV-PCM) system in hot climate. Solar Energy. 2017 Apr 1;146:417-29.

[67] Vidalain G, Gosselin L, Lacroix M. An enhanced thermal conduction model for the prediction of convection dominated solid–liquid phase change. International Journal of Heat and Mass Transfer. 2009 Mar 1;52(7-8):1753-60.

[68] Hendricks J, Sark W. Annual performance enhancement of building integrated photovoltaic modules by applying phase change materials. ProgPhotovolt Res Appl2013;21:620–30.

[69] Kuravi S, Trahan J, Goswami DY, Rahman MM, Stefanakos EK. Thermal energy storage technologies and systems for concentrating solar power plants. Progress in energy and combustion science. 2013 Aug 1;39(4):285-319.

[70] Du D, Darkwa J, Kokogiannakis G. Thermal management systems for photovoltaics (PV) installations: a critical review. Solar Energy. 2013 Nov 1;97:238-54.

[71] Ciulla G, Brano VL, Cellura M, Franzitta V, Milone D. A finite difference model of a PV-PCM system. Energy Procedia. 2012 Jan 1;30:198-206.

[72] Brano VL, Ciulla G, Piacentino A, Cardona F. Finite difference thermal model of a latent heat storage system coupled with a photovoltaic device: description and experimental validation. Renewable Energy. 2014 Aug 1;68:181-93.

[73] Zhou Z, Zhang Z, Zuo J, Huang K, Zhang L. Phase change materials for solar thermal energy storage in residential buildings in cold climate. Renewable and Sustainable Energy Reviews. 2015 Aug 1;48:692-703.

[74] Ma T, Yang H, Zhang Y, Lu L, Wang X. Using phase change materials in photovoltaic systems for thermal regulation and electrical efficiency improvement: A review and outlook. Renewable and Sustainable Energy Reviews. 2015 Mar 1;43:1273-84.

[75] Kant K, Shukla A, Sharma A, Biwole PH. Heat transfer studies of photovoltaic panel coupled with phase change material. Solar Energy. 2016 Dec 15;140:151-61.

[76] Bahaidarah HM, Baloch AA, Gandhidasan P. Uniform cooling of photovoltaic panels: A review. Renewable and Sustainable Energy Reviews. 2016 May 1;57:1520-44.

[77] Ma T, Zhao J, Han J. A parametric study about the potential to integrate phase change material into photovoltaic panel. Energy Procedia. 2017 Dec 1;142:648-54.

[78] Ma T, Zhao J, Li Z. Mathematical modelling and sensitivity analysis of solar photovoltaic panel integrated with phase change material. Applied Energy. 2018 Oct 15;228:1147-58.

[79] Zhao J, Ma T, Li Z, Song A. Year-round performance analysis of a photovoltaic panel coupled with phase change material. Applied Energy. 2019 Jul 1;245:51-64.

[80] Ma T, Li Z, Zhao J. Photovoltaic panel integrated with phase change materials (PV-PCM): technology overview and materials selection. Renewable and Sustainable Energy Reviews. 2019 Dec 1;116:109406.

[81] Savvakis N, Dialyna E, Tsoutsos T. Investigation of the operational performance and efficiency of an alternative PV- PCM concept. Solar Energy. 2020 Nov 15;211:1283-300.

[82] Sharma NK, Gaur MK, Malvi CS. Application of phase change materials for cooling of solar photovoltaic panels: A review. Materials Today: Proceedings. 2021 Jan 1;47:6759-65.

[83] Huang MJ. The effect of using two PCMs on the thermal regulation performance of BIPV systems. Solar Energy Materials and Solar Cells. 2011 Mar 1;95(3):957-63.

[84] Hudisteanu S, Mateescu TD, Chereches NC, Popovici CG. Numerical study of air cooling photovoltaic panels using heat sinks. RevistaRomana de InginerieCivila. 2015;6(1):11.

[85] Japs E, Sonnenrein G, Krauter S, Vrabec J. Experimental study of phase change materials for photovoltaic modules: Energy performance and economic yield for the EPEX spot market. Solar energy. 2016 Dec 15;140:51-9.

[86] Barroso JS, Barth N, Correia JP, Ahzi S, Khaleel MA. A computational analysis of coupled thermal and electrical behavior of PV panels. Solar Energy Materials and Solar Cells. 2016 Apr 1;148:73-86.

[87] Sharfabadi M, Ghiasi MI, Seraj A. Energy and Exergy Analysis of 190 W Photovoltaic Cell. Mechanical Engineering. 2021 Jan 1;21(11):743-55.

[88] Siddiqui MU, Arif AF, Kelley L, Dubowsky S. Three-dimensional thermal modeling of a photovoltaic module under varying conditions. Solar energy. 2012 Sep 1;86(9):2620-31.

[89] Tsai HL. Complete PV model considering its thermal dynamics. Journal of the Chinese institute of engineers. 2013 Dec 1;36(8):1073-82.

[90] Sarhaddi F, Farahat S, Ajam H, Behzadmehr A. Exergetic optimization of a solar photovoltaic array. Journal of Thermodynamics 2009;2009:1-11.

[91] Skoplaki E, Boudouvis AG, Palyvos JA. A simple correlation for the operating temperature of photovoltaic modules of arbitrary mounting. Solar energy materials and solar cells. 2008 Nov 1;92(11):1393-402.

[92] W. De Soto, Improvement and validation of a model for photovoltaic array performance, M.S. thesis, Solar Energy Laboratory, University of Wisconsin—Madison, Madison, Wis, USA, 2004.

[93] Sahin AD, Dincer I, Rosen MA. Thermodynamic analysis of solar photovoltaic cell systems. Solar energy materials and solar cells. 2007 Jan 23;91(2-3):153-9.

[94] A. S. Joshi, I. Dincer, and B. V. Reddy, "Thermodynamic assessment of photovoltaic systems," Solar Energy, vol. 83, no8, pp. 1139–1149, 2009.

[95] Seyyedi SM, Ajam H, Farahat S. A new criterion for the allocation of residues cost in exergoeconomic analysis of energy

systems. Energy. 2010 Aug 1;35(8):3474-82.

[96] T. J. Kotas, The Exergy Method of Thermal Plant Analysis, Krieger, Malabar, Fla, USA, 1995.

[97] Petela R. An approach to the exergy analysis of photosynthesis. Solar Energy. 2008 Apr 1;82(4):311-28.

[98] Petela R. Exergy of undiluted thermal radiation. Solar energy. 2003 Jun 1;74(6):469-88.

[99] Holmberg J, Flynn C, Portinari L. The colours of the Sun. Monthly Notices of the Royal Astronomical Society. 2006 Apr 1;367(2):449-53.

[100] Farahat S, Sarhaddi F, Ajam H. Exergetic optimization of flat plate solar collectors. Renewable energy. 2009 Apr 1;34(4):1169-74.

[101] Ajam H, Farahat S, Sarhaddi F. Exergetic optimization of solar air heaters and comparison with energy analysis. International Journal of Thermodynamics. 2005;8(4):183-90.

[102] J.A. Duffie, W.A. Beckman, Solar Engineering of Thermal Processes, fourth ed., John Wiley & Sons, Inc, Hoboken, New Jersey, U.S.A, 2013.

[103] Kaplani E, Kaplanis S. Thermal modelling and experimental assessment of the dependence of PV module temperature on wind velocity and direction, module orientation and inclination. Solar Energy. 2014 Sep 1;107:443-60.

[104] Mattei M, Notton G, Cristofari C, Muselli M, Poggi P. Calculation of the polycrystalline PV module temperature using a simple method of energy balance. Renewable energy. 2006 Apr 1;31(4):553-67.

[105] Khanna S, Reddy KS, Mallick TK. Performance analysis of tilted photovoltaic system integrated with phase change material under varying operating conditions. Energy. 2017 Aug 15;133:887-99.

[106] Aelenei L, Pereira R, Gonçalves H, Athienitis A. Thermal performance of a hybrid BIPV-PCM: modeling, design and experimental investigation. Energy Procedia. 2014 Jan 1;48:474-83.

[107] Biwole PH, Eclache P, Kuznik F. Phase-change materials to improve solar panel's performance. Energy and Buildings. 2013 Jul 1;62:59-67.

[108] Notton G, Cristofari C, Mattei M, Poggi P. Modelling of a double-glass photovoltaic module using finite differences. Applied thermal engineering. 2005 Dec 1;25(17-18):2854-77.

[109] Cole RJ, Sturrock NS. The convective heat exchange at the external surface of buildings. Building and Environment. 1977 Jan 1;12(4):207-14.

[110] Test FL, Lessmann RC, Johary A., Heat transfer during wind flow over rectangular bodies in the natural environment, J. Heat Transf. 103 (1981) 262–267, http://dx.doi.org/10.1115/1.3244451.

[111] A. Bejan, A.D. Kraus, Heat Transfer Handbook. Wiley-IEEE, 2003.801-808.

[112] F.P. Incropera, D.P. DeWitt, Fundamentals of Heat and Mass Transfer. John Wiley & Sons, 2002.

[113] Li Z, Ma T, Zhao J, Song A, Cheng Y. Experimental study and performance analysis on solar photovoltaic panel integrated with phase change material. Energy. 2019 Jul 1;178:471-86.

[114] Hachem F, Abdulhay B, Ramadan M, El Hage H, El Rab MG, Khaled M. Improving the performance of photovoltaic cells using pure and combined phase change materials–Experiments and transient energy balance. Renewable Energy. 2017 Jul 1;107:567-75.

[115] Hasan A, McCormack SJ, Huang MJ, Sarwar J, Norton B. Increased photovoltaic performance through temperature regulation by phase change materials: Materials comparison in different climates. Solar Energy. 2015 May 1;115:264-76.

[116] Kibria MA, Saidur R, Al-Sulaiman FA, Aziz MM. Development of a thermal model for a hybrid photovoltaic module and phase change materials storage integrated in buildings. Solar Energy. 2016 Feb 1;124:114-23.

[117] Klugmann-Radziemska E, Wcisło-Kucharek P. Photovoltaic module temperature stabilization with the use of phase change materials. Solar Energy. 2017 Jul 1;150:538-45.

[118] Zalba B, Marín JM, Cabeza LF, Mehling H. Review on thermal energy storage with phase change: materials, heat transfer analysis and applications. Applied thermal engineering. 2003 Feb 1;23(3):251-83.

[119] Sarhaddi F, Farahat S, Ajam H, Behzadmehr A. Exergetic performance assessment of a solar photovoltaic thermal (PV/T) air collector. Energy and Buildings. 2010 Nov 1;42(11):2184-99.

[120] Brahim T, Jemni A. Economical assessment and applications of photovoltaic/thermal hybrid solar technology: A review. solar Energy. 2017 Sep 1;153:540-61.

[121] Hissouf M, Najim M, Charef A. Numerical study of a covered Photovoltaic-Thermal Collector (PVT) enhancement using nanofluids. Solar Energy. 2020 Mar 15;199:115-27.

[122] Gu W, Ma T, Song A, Li M, Shen L. Mathematical modelling and performance evaluation of a hybrid photovoltaic-thermoelectric system. Energy Conversion and Management. 2019 Oct 15;198:111800.

[123] Luo Z, Zhu N, Hu P, Lei F, Zhang Y. Simulation study on performance of PV-PCM-TE system for year-round analysis. Renewable Energy. 2022 Aug 1;195:263-73.

[124] Lazaroiu GC, Longo M, Roscia M, Pagano M. Comparative analysis of fixed and sun tracking low power PV systems considering energy consumption. Energy Conversion and Management. 2015 Mar 1;92:143-8.

[125] Rahman MM, Hasanuzzaman M, Abd Rahim N. Effects of operational conditions on the energy efficiency of photovoltaic modules operating in Malaysia. Journal of cleaner production. 2017 Feb 1;143:912-24.

[126] Akal D, Türk S. Increasing energy and exergy efficiency in photovoltaic panels by reducing the surface temperature with thermoelectric generators. Energy Sources, Part A: Recovery, Utilization, and Environmental Effects. 2022 Jun 15;44(2):4062-82.

[127] Badescu V. Simple optimization procedure for silicon-based solar cell interconnection in a series–parallel PV module. Energy Conversion and Management. 2006 Jun 1;47(9-10):1146-58.

[128] Friling N, Jiménez MJ, Bloem H, Madsen H. Modelling the heat dynamics of building integrated and ventilated photovoltaic modules. Energy and Buildings. 2009 Oct 1;41(10):1051-7.

[129] Ikegami T, Maezono T, Nakanishi F, Yamagata Y, Ebihara K. Estimation of equivalent circuit parameters of PV module and its application to optimal operation of PV system. Solar energy materials and solar cells. 2001 Mar 1;67(1-4):389-95.

[130] De Soto W, Klein SA, Beckman WA. Improvement and validation of a model for photovoltaic array performance. Solar energy. 2006 Jan 1;80(1):78-88.

[131] Van Dyk EE, Gxasheka AR, Meyer EL. Monitoring current–voltage characteristics and energy output of silicon photovoltaic modules. Renewable Energy. 2005 Mar 1;30(3):399-411.

[132] Tiba C, Beltrão RE. Siting PV plant focusing on the effect of local climate variables on electric energy production–Case study for Araripina and Recife. Renewable Energy. 2012 Dec 1;48:309-17.

[133] Burns JE, Kang JS. Comparative economic analysis of supporting policies for residential solar PV in the United States: Solar Renewable Energy Credit (SREC) potential. Energy policy. 2012 May 1;44:217-25.

[134] Andrews RW, Pollard A, Pearce JM. Improved parametric empirical determination of module short circuit current for modelling and optimization of solar photovoltaic systems. Solar Energy. 2012 Sep 1;86(9):2240-54.

[135] Rehman S, El-Amin I. Performance evaluation of an off-grid photovoltaic system in Saudi Arabia. Energy. 2012 Oct 1;46(1):451-8.

[136] Sopian K, Ibrahim MZ, Daud WR, Othman MY, Yatim B, Amin N. Performance of a PV–wind hybrid system for hydrogen production. Renewable Energy. 2009 Aug 1;34(8):1973-8.

[137] Notton G, Diaf S, Stoyanov L. Hybrid photovoltaic/wind energy systems for remote locations. Energy Procedia. 2011 Jan 1;6:666-77.

[138] Vick BD, Neal BA. Analysis of off-grid hybrid wind turbine/solar PV water pumping systems. Solar Energy. 2012 May 1;86(5):1197-207.

[139] Masoum MA, Dehbonei H, Fuchs EF. Theoretical and experimental analyses of photovoltaic systems with voltageand current-based maximum power-point tracking. IEEE Transactions on energy conversion. 2002 Dec;17(4):514-22.

[140] Esram T, Chapman PL. Comparison of photovoltaic array maximum power point tracking techniques. IEEE Transactions on energy conversion. 2007 May 21;22(2):439-49.

[141] Nguyen DD, Lehman B. Modeling and simulation of solar PV arrays under changing illumination conditions. In2006 IEEE Workshops on Computers in Power Electronics 2006 Jul 16 (pp. 295-299). IEEE.

[142] JafariFesharaki V, Dehghani M, JafariFesharaki J, Tavasoli H. The effect of temperature on photovoltaic cell efficiency. InProceedings of the 1stInternational Conference on Emerging Trends in Energy Conservation–ETEC, Tehran, Iran 2011 Nov 20 (Vol. 20, pp. 20-21).

[143] Sudhakar K, Srivastava T. Energy and exergy analysis of 36 W solar photovoltaic module. International Journal of Ambient Energy. 2014 Jan 2;35(1):51-7.

[144] Aoun N, Nahman B, Chenni R. Study of Experimental Energy and Exergy of mono-crystalline PV Panel in Adrar Region, Algeria. International Journal of Scientific and Engineering Research. 2014;5(10):2229-5518.

[145] Bayrak F, Ertürk G, Oztop HF. Effects of partial shading on energy and exergy efficiencies for photovoltaic panels. Journal of cleaner production. 2017 Oct 15;164:58-69.

[146] Carmona M, Bastos AP, García JD. Experimental evaluation of a hybrid photovoltaic and thermal solar energy collector with integrated phase change material (PVT-PCM) in comparison with a traditional photovoltaic (PV) module. Renewable Energy. 2021 Jul 1;172:680-96.

[147] Rabie R, Emam M, Ookawara S, Ahmed M. Thermal management of concentrator photovoltaic systems using new configurations of phase change material heat sinks. Solar Energy. 2019 May 1;183:632-52.

[148] Riahi A, Ali AB, Fadhel A, Guizani A, Balghouthi M. Performance investigation of a concentrating photovoltaic thermal hybrid solar system combined with thermoelectric generators. Energy Conversion and Management. 2020 Feb 1;205:112377.

[149] Abdo A, Ookawara S, Ahmed M. Performance evaluation of a new design of concentrator photovoltaic and solar thermoelectric generator hybrid system. Energy Conversion and Management. 2019 Sep 1;195:1382-401.

[150] Motiei P, Yaghoubi M, GoshtasbiRad E. Transient simulation of a hybrid photovoltaic-thermoelectric system using a phase change material. Sustainable Energy Technologies and Assessments. 2019 Aug 1;34:200-13.

[151] Darkwa J, Calautit J, Du D, Kokogianakis G. A numerical and experimental analysis of an integrated TEG-PCM power enhancement system for photovoltaic cells. Applied Energy. 2019 Aug 15;248:688-701.

[152] Rajaee F, Rad MA, Kasaeian A, Mahian O, Yan WM. Experimental analysis of a photovoltaic/thermoelectric generator using cobalt oxide nanofluid and phase change material heat sink. Energy Conversion and Management. 2020 May 15;212:112780.

[153] Naderi M, Ziapour BM, Gendeshmin MY. Improvement of photocells by the integration of phase change materials and thermoelectric generators (PV-PCM-TEG) and study on the ability to generate electricity around the clock. Journal of Energy Storage. 2021 Apr 1;36:102384.

[154] Kosmadakis G, Manolakos D, Papadakis G. Simulation and economic analysis of a CPV/thermal system coupled with an organic Rankine cycle for increased power generation. Solar Energy. 2011 Feb 1;85(2):308-24.

[155] Zhao J, Li Z, Ma T, Performance analysis of a photovoltaic panel integrated with phasechange material, 10th International Conference on Applied Energy (ICAE2018), 22-25 August 2018, Hong Kong, China

[156] Rea JE, Oshman CJ, Olsen ML, Hardin CL, Glatzmaier GC, Siegel NP, Parilla PA, Ginley DS, Toberer ES. Performance modeling and techno-economic analysis of a modular concentrated solar power tower with latent heat storage. Applied energy. 2018 May 1;217:143-52.